Continental Shelf Research 110 (2015) 108–123

Contents lists available at ScienceDirect

Continental Shelf Research

journal homepage: www.elsevier.com/locate/csr

Event-to-seasonal sediment dispersal on the Waipaoa River Shelf, New Zealand: A numerical modeling study

Julia M. Moriarty [a,*], Courtney K. Harris [a], Mark G. Hadfield [b]

[a] Virginia Institute of Marine Science, The College of William & Mary, P.O. Box 1346, Gloucester Point, VA 23062, USA
[b] National Institute of Water and Atmospheric Research, 301 Evans Bay Parade, Hataitai, Private Bag 14 901, Wellington 6021, New Zealand

ARTICLE INFO

Article history:
Received 29 August 2014
Received in revised form
23 September 2015
Accepted 8 October 2015
Available online 14 October 2015

Keywords:
Sediment transport
Numerical model
Flood deposit
River dispersal
Wave resuspension
Waipaoa shelf
New Zealand

ABSTRACT

The formation of the geologic record offshore of small mountainous rivers is event-driven and, more so than many other environments, can result in relatively complete sequences. One such river, the Waipaoa in New Zealand, has been studied from its terrestrial source to its oceanic sink over timescales spanning storms, seasons, and the Holocene. This study focused on the formation of riverine deposits on the Waipaoa Shelf during episodic flood and wave events, contrasting deposition during short-lived events to accumulation patterns created over thirteen months. Sediment fluxes and fate were estimated using the numerical hydrodynamic and sediment transport model ROMS, the Regional Ocean Modeling System, using CSTMS, the Community Sediment Transport Modeling System. During the study period (January 2010–February 2011), the model indicated that initial flood deposition generally occurred near the river mouth and along the coast in water shallower than 40 m, and that deposition during any one event was sensitive to variations in shelf currents and wave energy. Also, the sedimentation due to plume settling and suspended transport during these relatively short flood and wave events were not aligned with longer time-scale accumulation patterns (months or greater) previously reported for the Waipaoa shelf. In the days to months following a flood pulse, waves episodically reworked this initial deposit, resuspending centimeter-scale layers of sediment during energetic periods. Frequent and intense resuspension occurred in shallow areas where bed stresses were high. This encouraged redistribution of material toward deeper areas having lower near-bed wave stresses, including continental shelf depocenters and offshore areas. While fast settling material was preferentially retained near the river mouth, currents dispersed slower settling sediment farther before deposition. Overall, accumulation depended on characteristics of oceanographic transport (wave energy, current velocities), not just source characteristics (flood size, sediment size distribution).

1. Motivation

The marine geologic record is incomplete, complicating interpretation of seabed observations (e.g. Sadler, 1981; Orpin et al., 2010). Flood deposits, for instance, comprise significant components of the geologic record on river-dominated margins, but are often reworked by physical and biological processes following initial emplacement (e.g. Wheatcroft et al., 2007). The resuspension and redistribution of fluvial sediment, the focus of this paper, can erase flood deposits from the stratigraphic record and likely impacts their significance as carbon sinks (Wheatcroft and Drake, 2003; Blair et al., 2004).

Wright and Nittrouer (1995) partition the dispersal of terrestrial material from rivers into four general dispersal stages: (I) supply of material via plumes; (II) initial deposition; (III) resuspension and transport by marine processes; and (IV) long-term net accumulation. In some situations, multiple stages may coincide. For example, initial deposition may occur during periods of supply via plumes and/or while energetic waves resuspend seabed material. In this paper, Stage I refers to the movement of the river plume and the associated fluxes of material. Stage II includes the location and characteristics of the deposit formed by the flood. Stage III refers to a period of seabed reworking and redistribution of material that begins after the flood-associated storm conditions have waned and flood sediments have had sufficient time to settle. For the Waipaoa Shelf this often begins within about 2 weeks after the flood, but can last for some years. Stage IV refers to deposition over decadal or longer timescales.

The relative importance of each dispersal stage varies among margins, but Wright and Nittrouer (1995) hypothesized that rapid initial deposition is especially dominant for small mountainous

* Corresponding author.
E-mail addresses: moriarty@vims.edu (J.M. Moriarty), ckharris@vims.edu (C.K. Harris), mark.hadfield@niwa.co.nz (M.G. Hadfield).

http://dx.doi.org/10.1016/j.csr.2015.10.005

rivers. Recent studies have shown that geologic records offshore of small mountainous rivers may have relatively good fidelity, meaning that deposits formed by specific events can be preserved in the marine sedimentary record (e.g. Sommerfield and Nittrouer, 1999; Wheatcroft et al., 2007; Blair et al., 2004; Brackley et al., 2010; Selvaraj et al., 2015). Certain characteristics of these river-dominated active margins, e.g. the rivers' small drainage basins, high sediment yield, and steep slopes, encourage this fidelity by helping to deliver signals from terrestrial flood events to the coastal ocean in coherence with the storm conditions that caused the rain and associated high discharge (Milliman and Syvitski, 1992; Wheatcroft, 2000). Upon reaching the continental shelf, steep slopes, combined with energetic waves and currents associated with the storm, may help sediment transit quickly to deeper sites where wave resuspension is less likely, enhancing preservation of flood deposits (Wright and Friedrichs, 2006; Wiberg, 2000; Warrick and Milliman, 2003). Although this paradigm fits many small mountainous rivers (e.g. the Eel River: Traykovski et al., 2000; Harris et al., 2005; the Gaoping River: Selvaraj et al., 2015; the Santa Clara River: Warrick et al., 2008), recent field data and model results for the Waipaoa River shelf have implied that event layer formation is not necessarily coherent with flood conditions. Instead, the Waipaoa shelf record reflects reworking by oceanographic transport mechanisms, and only the largest floods and storms would leave a preservable event bed there (Walsh et al., 2014; Bever and Harris, 2014; Rose, 2012).

Despite the relatively good fidelity and notable terrestrial influence expected offshore of small mountainous rivers, physical and biological processes are known to rework deposits on river-dominated margins (Wright and Nittrouer, 1985's Dispersal Stage III). On continental shelves, the impact of reworking on event layer preservation varies with depth into the seabed and water depth. For instance, both biological and physical processes act primarily on near-surface sediments, so rapid burial of event layers enhances the preservation of distinct beds in the geologic record (Wheatcroft, 1990; Bentley and Nittrouer, 2003; Wheatcroft and Drake, 2003). Similarly, wave orbital velocities attenuate with water depth, so waves more effectively resuspend sediment in shallow water (e.g. Harris and Wiberg, 2002). However, the temporal and spatial variability of these processes complicates efforts to estimate the likelihood of preservation for a given event deposit. Here, we investigated the role of physical reworking on the formation and preservation of continental shelf flood deposits and how patterns of fluvial accumulation, or net deposition, change on timescales of days to months.

This study focused on the Waipaoa River continental shelf, New Zealand, as part of the Waipaoa Source-to-Sink Studies. The National Science Foundation's (NSF) MARGINS program chose the Waipaoa as a Source-to-Sink focus site because it has a high sediment yield, interesting marine geologic record, and offshore anticlines that were thought to favor preservation of a relatively complete geologic record (see Fig. 1, Carter et al., 2010; Foster and Carter, 1997; Gomez et al., 2004; Hicks et al., 2000; Milliman and Farnsworth, 2011; Griffiths and Glasby, 1985; Hicks et al., 2004; Walling and Webb, 1996). However, previous studies, summarized in Kuehl et al. (2015), have indicated that physical processes (e.g. resuspension by waves, gravity-driven transport) likely affected variations (e.g. grain size, carbon signature) within the Waipaoa shelf geologic record (Bever, 2010; Brackley et al., 2010; Carter et al., 2010; Hale et al., 2014a). In spite of earlier studies, questions have remained about the role that transport processes play in sedimentation and event layer preservation on the shelf, and how short-term deposition differs from long-term accumulation. This numerical modeling study addressed these questions by estimating sediment fluxes and deposition over the entire shelf for a thirteen-month period that coincided with a field experiment (described below) and included two floods and multiple wave events.

1.1. Waipaoa sedimentary system

The Waipaoa River, a small mountainous river with a highly erodible catchment, delivers sediment to the coastal ocean primarily during floods (Orpin et al., 2006; Hicks et al., 2000). The riverine load is primarily mud (D_{50}=8.5 μm during floods), although sands comprise about one percent of the fluvial load (Hicks et al., 2004; Orpin et al., 2006). This paper focuses on the period from January 2010–February 2011, which overlaps with associated field studies (i.e. Hale et al., 2014a; Walsh et al., 2014; Kniskern et al., 2014; Kiker, 2012; Fig. 1b). During this time, two large Waipaoa River floods occurred on January 31 and July 6, 2010 that represented the fifth and fourteenth largest discharges, respectively, in the 44-year record of Waipaoa River observations provided by the Gisborne District Council (GDC). Riverine sediment concentrations during the peaks of these floods were estimated to slightly exceed 40 g L^{-1} based on recent rating curves provided by

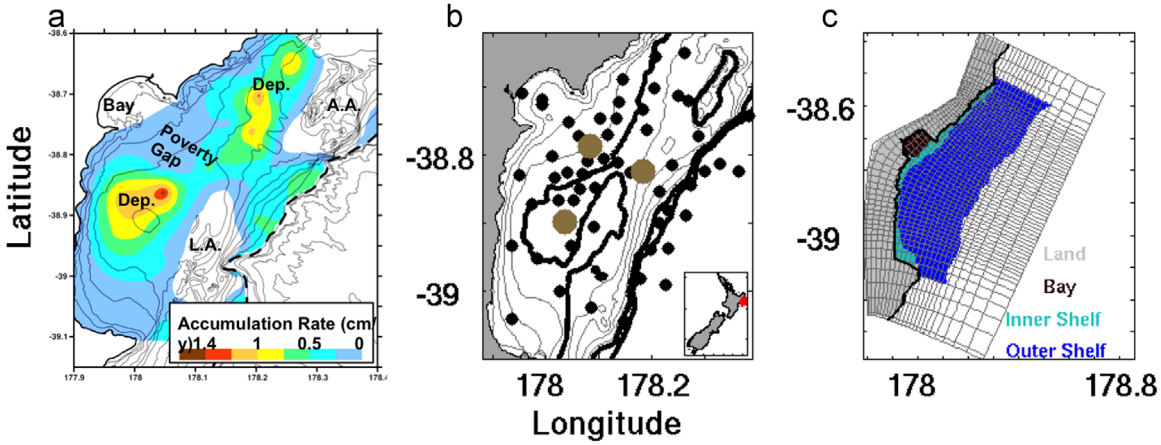

Fig. 1. Study site on North Island, New Zealand. (a) Adapted from Miller and Kuehl (2010). Spatial distribution of accumulation rates (cm y^{-1}) based on ^{210}Pb. Labels identify the Waipaoa River (red arrow), Poverty Bay (Bay), Poverty Gap, Lachlan Anticline (L.A.), Ariel Anticline (A.A.), and depocenters (Dep.). Bathymetric contours mark every 10 m (gray line) and the shelf break (black, dashed line). (b) Waipaoa Shelf map showing tripod locations (brown) and multi-core stations (black) from the January, 2010 research cruise. Inset shows location of study site in New Zealand. Bathymetric contours mark every 10 m (gray) and 50 m (black) depth intervals. (c) Waipaoa model grid. Boxes each encompass 25 grid cells. Colors (red, light blue, blue) indicate areas for sediment budgets discussed in Sections 4 and 5 (For interpretation of the references to color in this figure legend,the reader is referred to the web version of this article).

the GDC.

The weather systems and hydrodynamics driving sediment dispersal on this margin are highly variable. In 2010, shelf currents generally flowed along shore (Hale et al., 2014a). Time- and depth-averaged velocities measured at 40 m water depth in Poverty Gap (see Fig. 1b) were 1.6 cm/s to the NE, but they switched direction frequently and had a mean speed of 26.3 cm/s (data from Hale et al., 2014a). Several factors likely influenced currents, including a northward coastal current, coastally-trapped waves, and southward-traveling eddies (Chiswell, 2000; Wood, 2006; Stephens et al., 2000; Chiswell and Roemmich, 1998; Chiswell, 2005). Surface gravity waves generally approach the shelf from the southeast, and include longer-period swell from the Southern Ocean (Bever et al., 2011; Smith, 1988). The wave climate of the Waipaoa shelf is often energetic enough to suspend sediment. For example, estimated bed shear stresses from a tripod located at a water depth of 50 m exceeded 0.15 Pa, a conservative threshold for suspension of fine-grained sediment, 46% of the time during the 2010 field observations (data from Hale et al., 2014a; see tripod location in Fig. 1b). This indicates that conditions were energetic enough to cause suspension there about half of the time.

Energetic waves and winds on the Waipaoa shelf generally coincide with southward-traveling storms that also cause river floods (Orpin et al., 2006). Although winds are predominantly from the north-northwest (seaward), storms typically bring strong winds that blow shoreward during peak discharge, but then relax and change direction (Stephens et al., 2000; Orpin et al., 2006). Noting this, Orpin et al. (2006) and Bever et al. (2011) identified distinct phases during a typical discharge event of the Waipaoa River: Phase 1. Winds blow strongly shoreward during the rising limb of the flood; Phase 2. Winds rotate seaward during peak discharge and flood waning. Bever et al. (2011) further divided the second phase into a period of weak rotating winds, followed by a period of strong seaward winds that would act to decrease the energy of the generally southeastern storm waves. While winter (i.e. March–September) is the stormy season, some of the largest historical floods have happened during other times of year (Orpin et al., 2006). For example, the largest recorded flood, Cyclone Bola, occurred in March, 1988 and one of the biggest floods of our study period was in late January, 2010. In context, the 2010 field season was a relatively wet year for the watershed (Orpin, pers. comm., 2011), and the Waipaoa River experienced multiple periods of high discharge (wet storms), as well as wave events that did not coincide with precipitation or discharge (dry storms).

Sedimentation patterns formed over relatively short timescales on the Waipaoa shelf, e.g. during individual flood or wave resuspension events (Walsh et al., 2014; Kniskern et al., 2014), however, differ from those created by long-term accumulation. Typically, sediments delivered by floods are retained in the bay for several days before being resuspended by waves and exported to the shelf by currents, although gravity-driven processes can enhance offshore flows during large floods (Bever and Harris, 2014; Bever et al., 2011). On the shelf, recent data obtained during five coring expeditions over a period of thirteen months indicated that the locus of high deposition varies. Although the cruises were only separated by a few months, they saw that peak recent deposition shifted between different areas including near the river mouth in Poverty Bay, on the inner- to mid-shelf near the entrance to Poverty Bay, and in the long-term depocenters (Walsh et al., 2014; Kniskern et al., 2014). Over longer timescales, however, grain size measurements, ^{210}Pb (half-life equals 22.3 years) accumulation rates, and geophysical mapping have identified two mid-shelf (40–70 m water depth) depocenters that have actively accumulated sediment over century-long to Holocene timescales, that are bordered by anticlines on their seaward edge, and that are separated from each other by an area of low accumulation called Poverty Gap; (Fig. 1; Foster and Carter, 1997; Miller and Kuehl, 2010; Orpin et al., 2006). Although the sediment budget for shorter timescales has been difficult to determine (Kniskern et al., 2014; Walsh et al., 2014), about 25% of Waipaoa riverine sediment seems to remain on the shelf on century-long timescales, (Miller and Kuehl, 2010). This disconnect between the short-term and longer-term patterns may in part result from the reliance on discrete point observations that do not resolve spatial and temporal variability. Here, we use a numerical model to investigate this variability of sediment transport patterns across the shelf and over timescales of days to months; and to evaluate how delivery of sediment to the shelf, and the formation and preservation of event layers there, are influenced by both riverine and oceanographic (i.e. waves and currents) processes.

2. Objectives

This paper evaluates the roles that riverine and oceanic processes play in the dispersal of fluvially-derived sediment on the continental shelf of the Waipaoa Sedimentary System. Other studies of transport processes on the Waipaoa continental shelf have been limited to the analysis of data obtained from a few discrete locations (i.e. Hale et al., 2014a). By using a numerical model, we estimate sediment fluxes for the entire shelf, including locations not sampled by the field experiment. Specifically, our objectives were to:

- Characterize suspended sediment flux and deposition under diverse conditions. How does dispersal vary among different types of events, including a flood coinciding with relatively low wave energy, a series of subsequent dry wave events, a flood coinciding with high wave energy, and a series of subsequent wet wave events?
- Evaluate the roles of initial flood deposition and subsequent reworking on sediment accumulation patterns and characterize how these dispersal stages contributed to sediment accumulation over the thirteen-month study period. To what extent were initial flood deposits reworked by waves and currents?
- Explore the degree to which observations of long-term deposition can be related to depositional patterns and oceanographic conditions from the modeling study that encompassed about one year.

3. Methods

A numerical circulation and sediment transport model, ROMS – CSTMS (Regional Ocean Modeling System – Community Sediment Transport Modeling System) was developed for the Waipaoa River continental shelf, and evaluated using hydrodynamic and seabed observations, as described in Moriarty et al. (2014). Here, we used that model to investigate sediment transport and deposition for January 1, 2010– February 15, 2011 over a range of timescales. Estimates of sediment flux and deposition during floods, wave events, and the year as a whole were analyzed. This section briefly reviews the model formulation described more fully in Moriarty et al. (2014), and provides details of the model analysis.

3.1. Model description

ROMS, an open-source community model, solves the Navier–Stokes, continuity, and tracer advective-diffusion equations (Haidvogel et al., 2000; Haidvogel et al., 2008; Shchepetkin and McWilliams, 2005, 2009). The model grid encompassed the continental shelf and Poverty Bay offshore of the Waipaoa River,

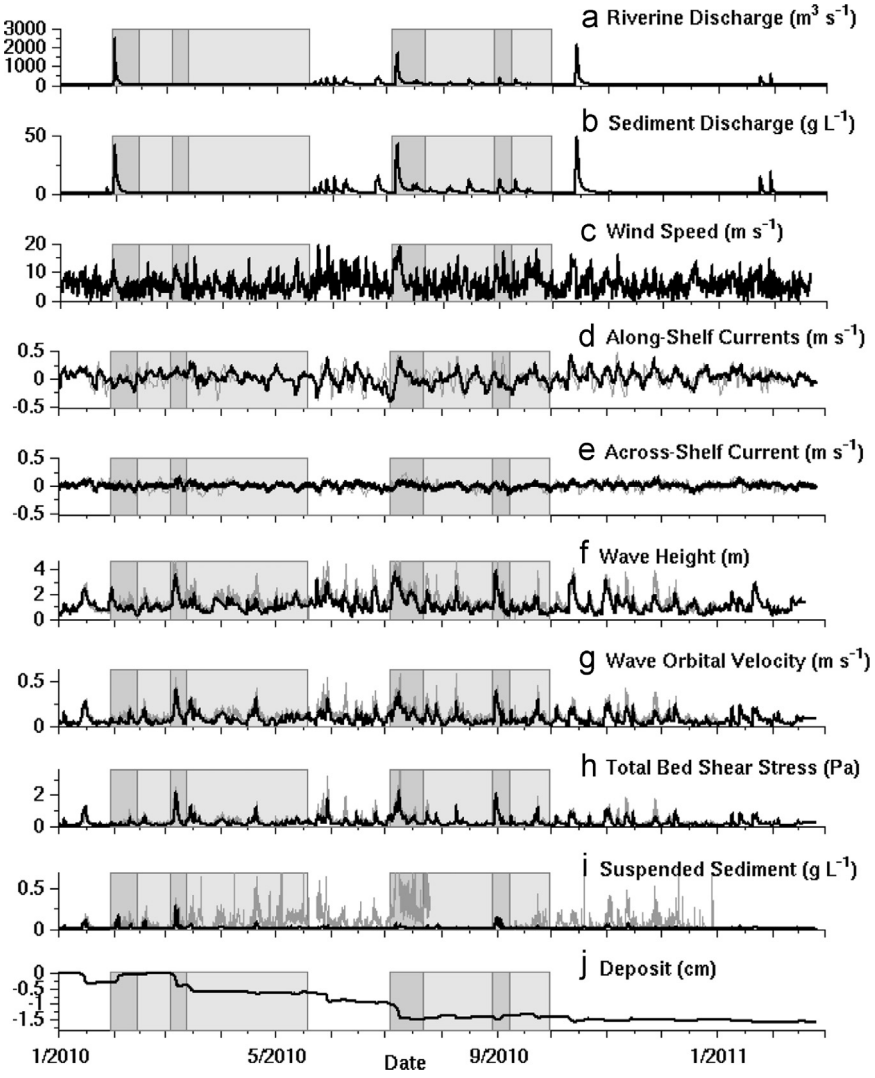

Fig. 2. Time series of conditions on the Waipaoa Shelf. (a) River and (b) sediment discharge from Gisborne District Council, New Zealand, (c) modeled wind speed from NZLAM averaged over the model domain, (d) along-isobath and (e) across-isobath depth-averaged tidally-filtered currents, (f) significant wave height, (g) wave orbital velocity, (h) total wave- and current- induced bed shear stress, (i) suspended sediment concentrations, and (j) seabed height calculated based on fluxes of fluvial and seabed material. Panels (d)–(j) include model estimates (black lines), and observations (gray lines) from acoustic Doppler current profilers (depth-averaged currents), acoustic Doppler velocimeters (wave height; bed shear stress) and optical backscatter sensors (suspended sediment concentration) observations (gray lines) from the shallow tripod site (Hale et al., 2014a; see Fig. 1b). For panels (d) and (e), positive values are to the northeast and offshore, respectively. Shaded boxes highlight events (dark gray) and periods of reworking following floods (light gray). Events include the January flood (1/30/2010–2/14/2010), March wave event (3/4/2010–3/13/2010), July flood (7/4/2010–7/22/2010), and August wave event (8/29/2010–9/8/2010). Periods of reworking include a time with dry wave events (2/15/2010–5/19/2010), and a time with wet wave events (7/22/2010–9/30/2010).

including the shelf and slope depocenters (Fig. 1). Horizontal grid resolution was highest, about 450 m, near shelf depocenters. ROMS uses a stretched, terrain-following vertical grid, so vertical resolution varied with water depth; it increased in shallow water, near the bed, and near the water surface. At 50 m water depth, grid cell thickness was 0.84 m near the seabed and water surface, and 5.3 m in the mid-water column. The ROMS implementation relied on a variety of observations and model estimates (see Fig. 2; Moriarty et al., 2014). To account for larger scale shelf currents, reduce reflection of the river plume at open boundaries, and ensure model stability, the model was nested within a larger scale New Zealand circulation model (similar to Hadfield et al., 2007; see Moriarty et al., 2014).

CSTMS, an open-source community model available as a module within ROMS, was used to estimate suspended sediment transport and deposition. As described in Warner et al. (2008), the model accounted for advection, diffusion, erosion and deposition of sediment. Both fluvial discharge and seabed erosion provided sediment sources to the water column. Seabed erosion was calculated following the Ariathurai and Arulanandan (1978) formulation:

$$E = M \bullet (1 - p) \bullet (\tau_{bed} - \tau_{crit}) / \tau_{crit} \quad (1)$$

where M was the erosion rate parameter, p was seabed porosity, τ_{bed} was bed shear stress, and τ_{crit} was critical bed shear stress. As explored in Moriarty et al. (2014), the erosion rate parameter (M) varied in space, and decreased with water depth from 4.5×10^{-4} to 0.1×10^{-4} kg m^{-2} s^{-1}. Wave- and current-induced bed stress was calculated following Madsen (1994) using a hydraulic roughness, z_o, of 0.03 cm and a bottom roughness length, k_n, of 0.9 cm to match estimates of bed shear stress from tripod observations (Moriarty et al., 2014). The density equation of state included sediment concentration to account for gravity-driven transport within the water column, to the degree afforded by the vertical resolution of the model.

The model accounted for seven sediment types and eight

seabed layers (see Moriarty et al., 2014). Four classes represented sediment delivered by the river and three classes represented sediment from the seabed. Settling velocities ranged from 0.15–1.0 mm s^{-1} for riverine material and a critical shear stress of 0.15 Pa was used for all sediment classes. The choice of settling velocity, critical shear stress, and other parameters were discussed in Moriarty et al. (2014), while Section 5.1 further explores model sensitivity to these sediment and seabed parameters.

3.2. Model analysis

This paper analyzes spatial and temporal variations in sediment transport and deposition on the Waipaoa shelf for four specific episodes, and then compares these event-timescale values to sedimentation patterns for the year as a whole. Specifically, the paper analyzes conditions during (1) a flood with relatively low waves on January 31, 2010; (2) a series of subsequent dry wave events (typical of summer conditions) with peak shelf sediment fluxes on March 7, 2010 when wave orbital velocities exceeded the thirteen-month average by a factor of 1.8; (3) a flood with high waves on July 6, 2010; and (4) a series of moderate discharge and wave events (typical of winter conditions) with peak shelf sediment fluxes on August 31, 2010 when orbital velocities reached about 1.6 times the thirteen-month average (Fig. 2; Table 1). The estimated transport and sedimentation patterns for each of these individual time periods (Section 4.1) are then compared to those of the entire thirteen-month model run (Section 4.2).

Although model calculations included both fluvial and seabed sediments, this analysis focused on the dispersal of the riverine material, unless otherwise noted. Throughout the paper, sediment budgets were calculated by integrating all of the fluvial sediment deposited and suspended in Poverty Bay and on the shelf. Note that 'shelf' refers to the continental shelf proximal to the Waipaoa River up to 150 m water depth, as indicated in Fig. 1c. The mass of the riverine load exported from the shelf was calculated by subtracting the sediment in Poverty Bay and on the shelf from the cumulative fluvial sediment input. Because settling velocities were difficult to constrain with the available data from the Waipaoa River and shelf, we provided estimates of dispersal for different classes of material whose settling velocities ranged from 0.15–1 mm/s (Fig. 3; Table 2). Ranges in sediment budgets presented here were based on estimates from the different sediment classes. Sediment fluxes were calculated as depth-integrated estimates, unless otherwise noted.

4. Results

This section describes the hydrodynamic climate and sediment dispersal patterns for the four focus events identified in Fig. 2 and Table 1 (Section 4.1), and for the 2010 study period as a whole (Section 4.2).

4.1. Sedimentation during floods and subsequent wave events

Large fluxes that occurred during relatively short episodes dominated sediment transport on this shelf. This section analyzes model results from the various types of events that produced large sediment fluxes, emphasizing how sediment dispersal responded to meteorological and oceanographic conditions. Sub-sections 4.1.1–4.1.4 describe, in chronological order, the model estimates for each of the four focus periods identified in Table 1. More specifically, Sub-sections 4.1.1 and 4.1.3 examine initial deposition of material during two floods, which illustrate Wright and Nittrouer's (1995) Dispersal Stages I and II. Sub-sections 4.1.2 and 4.1.4 describe the resuspension and redistribution of the riverine load during subsequent months, focusing on the wave events that dominated non-flood sediment fluxes, i.e. Wright and Nittrouer's (1995) Dispersal Stage III.

4.1.1. Sedimentation during a flood with relatively low waves

Here, we characterize sediment transport and initial deposition during a period of high discharge but low wave energy (i.e. Wright and Nittrouer's (1995) Dispersal Stages I and II), focusing on a two-week period (1/31/2010–2/14/2010) that included a large summer flood. During this January 31 flood, the wind- and Coriolis- driven river plume, superimposed on a larger-scale southwestward shelf current, spread sediment over a wide area. Initially, westward winds trapped a lot of the plume within Poverty Bay, although some water and sediment escaped the bay to the southwest (Fig. 4a). As winds shifted direction and weakened after peak flood, the plume turned offshore and then toward the northeast (Fig. 4b and c). Finally, in the days following peak flood as winds became variable in strength and direction, the larger-scale current directed the freshwater toward the south (Fig. 4d). In response to

Table 1
Modeled hydrodynamic conditions at the Poverty Gap tripod at 60 m water depth for different time periods (see Fig. 1b for location).

	Dates	Wave orbital velocity (cm/s)	Bed stress (Pa)	Current speed (cm/s)	Current direction (degrees[1])	Wind speed (m/s)	Wind direction (degrees[1])
Large Discharge Events, see Results Sections 4.1.1 and 4.1.3:							
January Flood	1/30/10–2/14/10	2.94	0.05	5.4	−161	5.4	−173
July Flood	7/4/10–7/22/10	8.29	0.28	14.3	75	8.7	78
Non-Flood Periods, see Results Sections 4.1.2 and 4.1.4:							
Summer Dry Waves	2/15/10–5/19/10	5.13	0.14	10.3	66	6.1	−89
Early March Wave Event	3/4/10–3/13/10	7.94	0.22	8.8	73	7.6	81
Winter Wet Waves	7/22/10–9/30/10	4.36	0.12	10.0	167	6.9	−44
Late August Wave Event	8/29/10–9/8/10	6.77	0.18	7.4	170	8.2	8.6
Entire Field Season; see Results Section 4.2							
Entire Field Season	1/15/10-2/15/11	4.30	0.13	11.2	75	6.6	−56

[1] Direction is given in degrees counterclockwise from east, toward which the currents and winds are traveling. Note that the wind direction is opposite to the normal convention for winds.

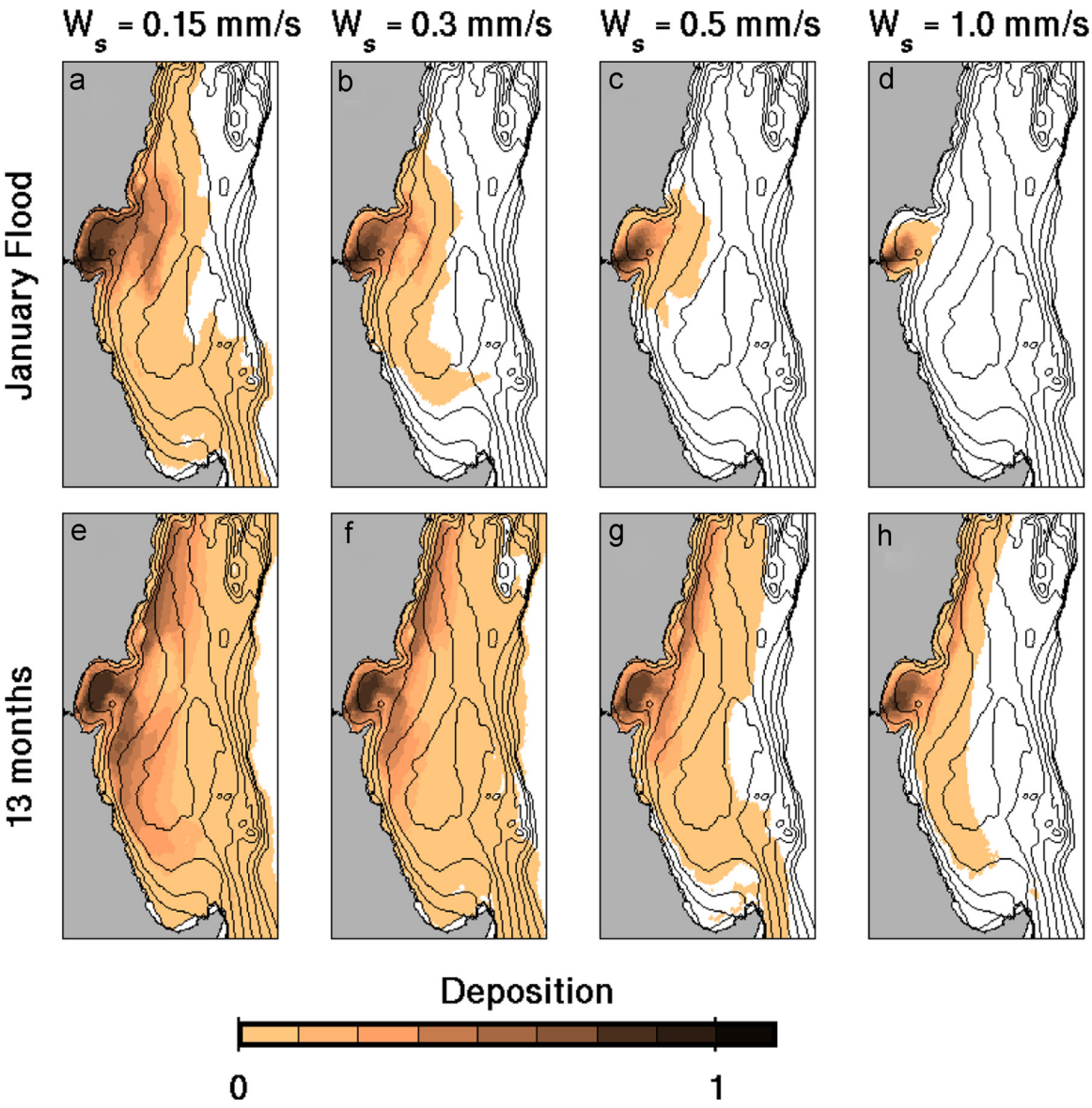

Fig. 3. Deposit thickness by sediment class calculated following the January flood for February 15, 2010 (a)–(d), and at the end of the field season on February 15, 2011 (e)–(h). To compare deposition among sediment classes that comprise different percentages of the total riverine load (see Table 2) and among different time periods for which cumulative riverine input varies, deposition is plotted on a scale from zero to one, with one equal to the thickest deposit estimated for that particular sediment class and time.

Table 2
Sediment budget for riverine sediments.

Grain size class	% of Riverine load	Settling velocity (mm/s)	% of Riverine load remaining in		
			Poverty Bay[1]	Shelf (outside of Poverty Bay)[1]	Transported offshore[1]
4	53	0.15	53	21	26
5	27	0.3	79	13	8
6	13	0.5	91	6	2
7	7	1.0	98	1	0

[1] Budgets were computed as follows: the total mass of suspended and deposited sediment in Poverty Bay and on the shelf (excluding Poverty Bay) was divided by the cumulative sum of sediment entering the model grid between 1 January 2010 and 15 February 2011. The remainder of sediment, including material transported out of the model to the northeast or southwest, was assumed to be transported 'offshore'.

the variable wind and plume trajectories, sediment fluxes during Dispersal Stage I and II of this event fluctuated (Figs. 4e and 5a).

The resulting flood deposit was focused in Poverty Bay and spread radially from the river mouth (Fig. 5a). Wave orbital velocities and bed stresses were relatively low, only reaching 40–70% of their average values (Fig. 5b). Thus, limited resuspension occurred during this flood, and sedimentation during this time was dominated by Wright and Nittrouer's Dispersal Stages I and II. Little of the riverine load escaped the shelf, but some of the slowly settling material reached deeper water, while the faster settling sediment remained close to the river mouth (Fig. 3). Over 99% of sediment with settling velocity of 1 mm/s remained in Poverty Bay, while 20% of the material settling at 0.15 mm/s was exported to the shelf. Of the sediment deposited on the shelf, 50–75%, depending on settling velocity, settled in areas shallower than 30 m.

4.1.2. *Waves redistribute January 31 flood deposit*

Next, we analyzed the months following the January 31 flood

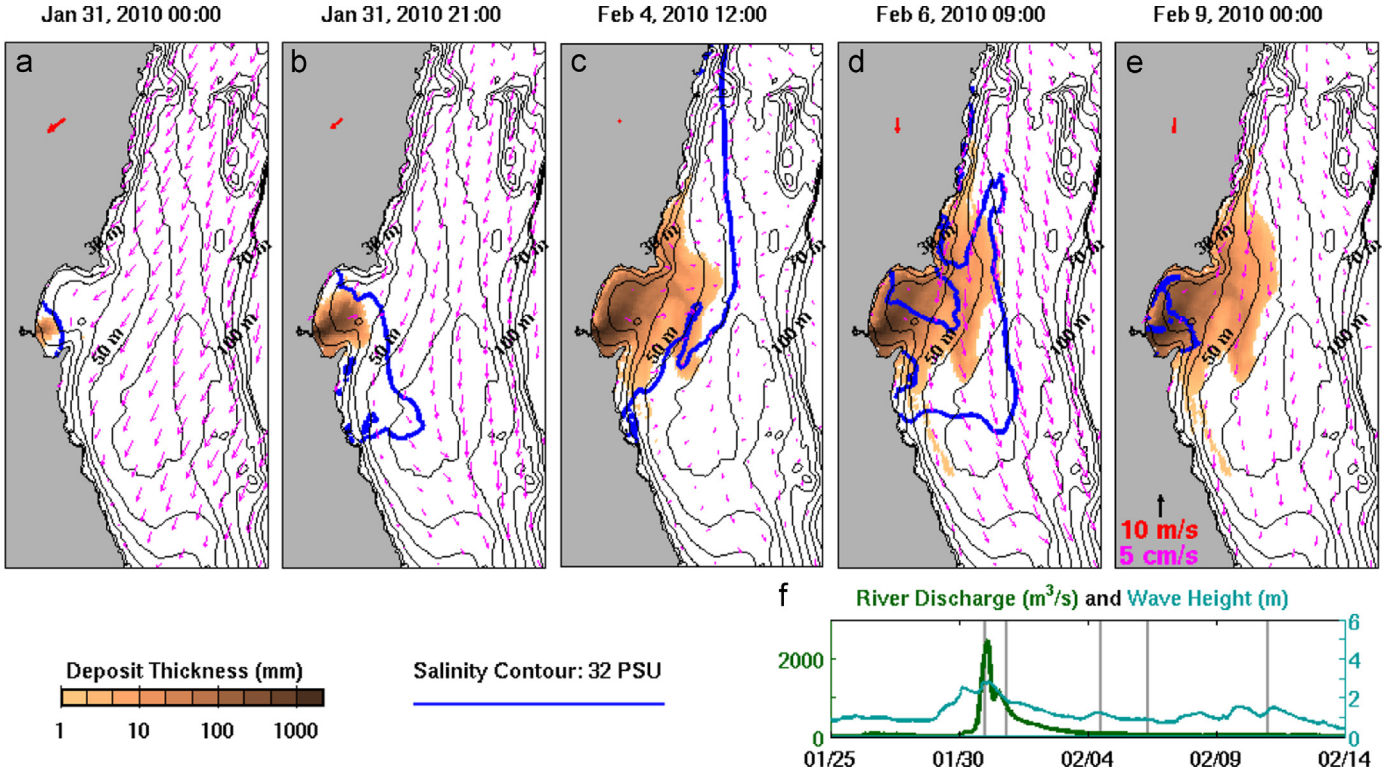

Fig. 4. January, 2010 flood 'snapshots' showing salinity contour (32 PSU) for surface waters (blue contours on maps), depth averaged currents (pink arrows), spatially-averaged wind (red arrow), and deposit thickness (brown shading on maps). Panels represent (a) early flood, (b) mid flood, during a time of onshore winds, (c) flood plume during a period of weak winds, (d) flood plume during a period of variable winds, and (e) post-flood. The gray lines on the time series of river discharge (dark blue) and wave height (turquoise) in panel (f) indicate the timing of the snapshots in (a)–(e) (For interpretation of the references to color in this figure legend, the reader is referred to the web version of this article).

(2/14/2010–5/15/2010) to evaluate the role of post-depositional reworking (i.e. Stage III dispersal). This three month period was characterized by several modest storms with wave heights of ~2 m, punctuated by a brief period of more intense waves around March 7, 2010 (3/4/2010–3/13/2010) during which peak wave height briefly exceeded 4 m (Fig. 2f). Characterized as "dry storms", these wave events occurred in the absence of precipitation, during a time of low river discharge (Fig. 2a).

Sediment fluxes for this three-month period were dominated by the March wave event. This 10-day period accounted for about three-fourths of the cumulative export from Poverty Bay to the Shelf, and about four-fifths of the cumulative export off of the proximal shelf, that occurred during the three months following the January flood. During this March event, wave-induced bed stresses were sufficiently strong to resuspend sediment across the entire shelf. Wave orbital velocities and bed stresses on the shelf exceeded their thirteen-month averages by about factors of ~1.7 and 1.8, respectively (Table 1). During this 10-day period of resuspension, currents exported up to 6% of the initial January flood deposit from Poverty Bay to the shelf (Fig. 5c). Strengthened by northward winds, shelf currents transported sediment to the northeast (Fig. 5d), exporting as much as 20% of some riverine sediment classes from the model grid. This dry storm caused net erosion in Poverty Gap, while northeastward currents facilitated net deposition north of this erosional area.

To a lesser extent than the energetic March wave event, additional small to moderate waves contributed to reworking of riverine sediments throughout the period from February 14, 2010 to May 15, 2010. Wave heights exceeded 1.5 m in 10 instances during these three months, including the large March wave event (Fig. 2f). Wave orbital velocities and bed stresses averaged throughout this time slightly exceeded the thirteen-month average (Table 1), and the model estimated that the moderate wave events slightly modified the overall sediment budgets for the bay and shelf (Fig. 5e and f). They enabled export of up to an additional 2% of the deposit from Poverty Bay to the shelf, and as much as an additional 5% of the January 31 flood load from the shelf. During these months, net transport was northeastward, and shelf- and depth-averaged sediment fluxes were directed to the northeast about 50% of the time. By the beginning of May, the modeled deposit extended along the coast in both directions from the river mouth up to about 60 m water depth, and was more dispersed compared to the initial footprint from the January flood.

4.1.3. *Sedimentation during a flood with high waves*

We next analyzed sediment dispersal and deposition during a large flood that coincided with energetic waves, focusing on 7/4/2010–7/22/2010 and encompassing dispersal Stages I, II and III. The peak discharge of over 1700 $m^3 s^{-1}$ occurred on July 6, 2010. Wave orbital velocities reached about twice the thirteen-month average, energetic enough to resuspend sediment across the shelf (Fig. 2g). During the early phase of the flood, shoreward winds toward the northwest at the onset and peak of flooding trapped the river plume in Poverty Bay (Fig. 6a and b). Then, as the winds rotated toward the northeast following peak flood, the river plume and shelf currents also turned to carry sediment northeastward (Fig. 6c). This reinforced the northeastward tendency of the coastal current, and at times material was transported beyond the proximal shelf. In the days to weeks following the flood, river discharge and winds returned to background conditions. The riverplume mostly withdrew into Poverty Bay, although a period of onshore winds together with the eddy over the southern depocenter (Fig. 7b) caused the plume to flow to the southwest for about a day and a half before the region of freshwater influence withdrew

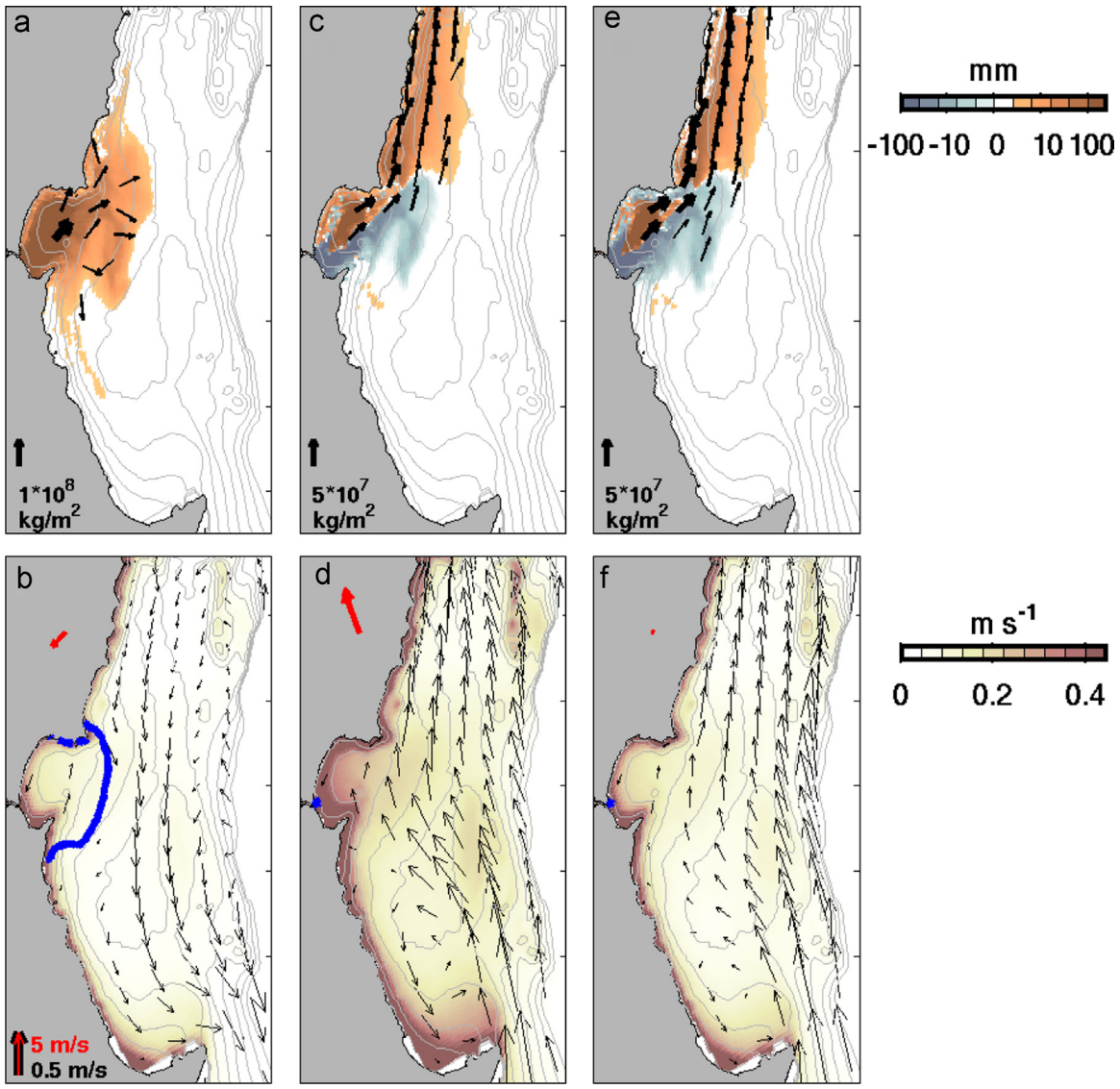

Fig. 5. Cumulative sediment fluxes and hydrodynamic conditions for time periods during and following the January flood. *Top*: Cumulative deposition (positive) and erosion (negative) of riverine sediments during specific time periods, shown when changes in seabed height exceed 1 mm. Flux arrows shown for every 10 grid cells where fluxes exceed 2×10^6 kg m^2, except as noted. Note difference in scale in (a) compared to (c), (e). *Bottom*: Time-averaged wave orbital velocities (shading), depth-averaged currents (black arrows), surface salinity (blue contour representing 32 ppt), and spatially-averaged wind (red arrow) during the time period. Currents shown for every 12 grid cells. Time periods include flood conditions (a) and (b) January 30–February 14, 2010; a short, energetic wave event (c) and (d) March 4–13, 2010; and months of moderate waves (e) and (f) February 14–May 15, 2010 (For interpretation of the references to color in this figure legend, the reader is referred to the web version of this article).

from the shelf into the bay (Fig. 6d and e). Overall, the combination of these currents created a net northward flux, dominated by surface transport. Near-bed currents in the model were usually aligned with water column velocities, but they had an increased offshore component during the flood when sediment concentrations and wave energy were high in Poverty Bay and the inner shelf. These near-bed currents, as well as, at times, an eddy over the southern depocenter and shoreward winds, enhanced southwestward fluxes.

During this flood, net sedimentation occurred in Poverty Bay and on the shelf, both to the north of the Waipaoa River in water up to ~50 m deep and landward of the southern depocenter in 30–55 m water depths (Fig. 7a). More than half of flood sediment deposited in Poverty Bay, and up to a third was carried off of the proximal shelf to the northeast. Settling velocity again controlled the model's partitioning of sediment on the shelf, with half of the fast settling (w_s=1.0 mm/s) and three-fourths of the slow settling (w_s=0.15 mm/s) material leaving Poverty Bay but remaining on the shelf and settling in areas deeper than 30 m.

4.1.4. Winter storms (discharge pulses and waves) redistribute flood deposit

In the two months following the July flood, a series of smaller discharge peaks coincided with energetic waves, delivering sediment to the shelf (Dispersal Stages I and II), and modifing the deposit footprint (Dispersal Stage III). During the timeframe of 7/22/2010–9/30/2010, six of these "wet storms" with discharge over 100 m^3 s^{-1} occurred, including a period of especially intense waves around August 31, 2010 (8/29–9/8/2010; Fig. 2a, b and f; Table 1).

The August 31 event, when river discharge peaked at just under 400 m^3 s^{-1} and wave orbital velocities exceeded the thirteen-month average by a factor of about 1.5 (Table 1), accounted for the largest sediment fluxes during the two months of wet storms. Altogether, these eleven days accounted for ~73% of the flux from Poverty Bay to the shelf during the months of wet storms. Resuspension occurred across the shelf, and near-bed currents in the mouth of Poverty Bay and the inner shelf carried sediment downslope from the bay toward the southern depocenter (Fig. 7c). On

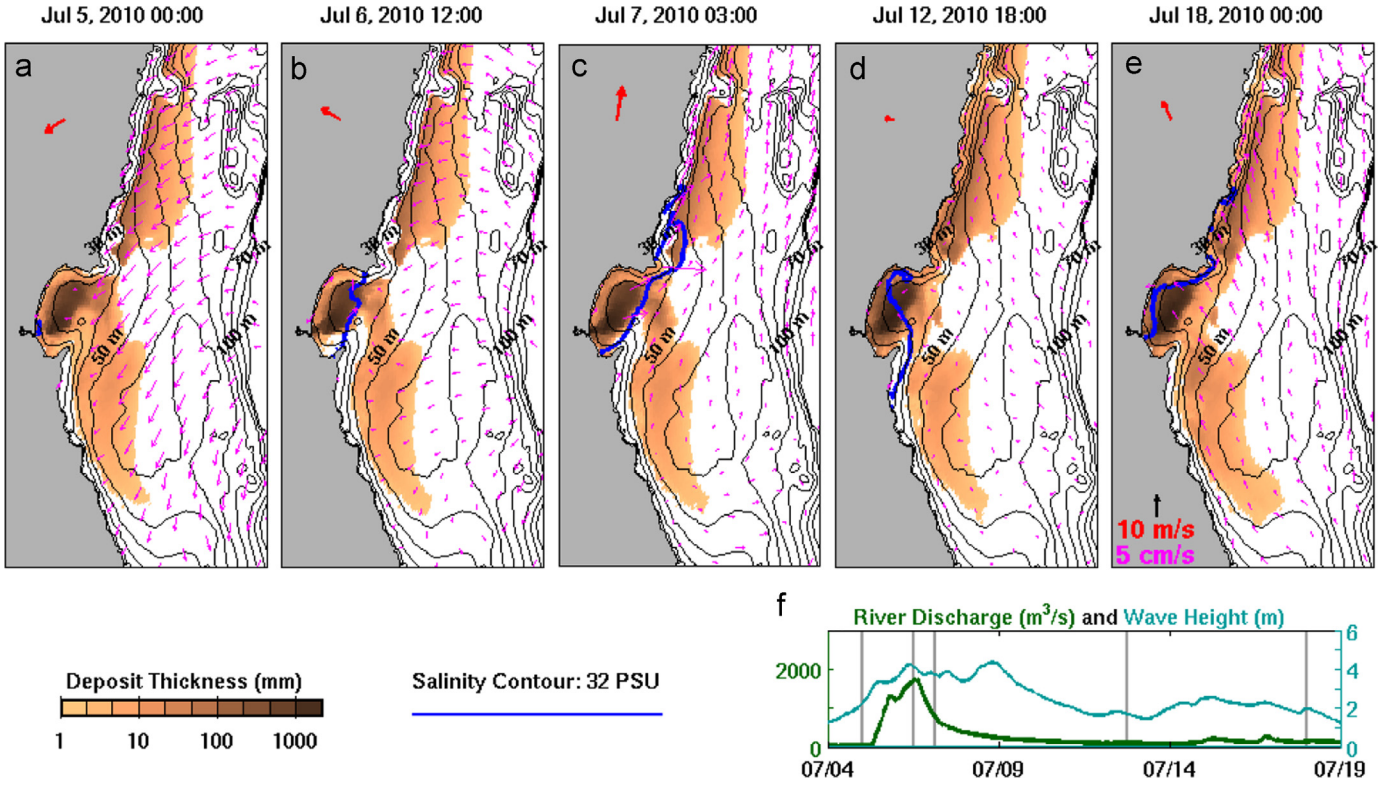

Fig. 6. Same as Fig. 4, but for the July, 2010 flood. Snapshots represent (a) early flood, (b) mid flood, during a time of onshore winds, (c) flood plume during a period of offshore, northeastward winds, (d) flood plume during a period of variable winds, and (e) post-flood. The gray lines on the time series of river discharge (dark blue) and wave height (turquoise) in panel (f) indicate the timing of the snapshots in (a)–(e) (For interpretation of the references to color in this figure legend, the reader is referred to the web version of this article).

the shelf, the river plume was trapped in the bay for most of this time period, but did briefly flow northward, driven by the Coriolis effect and wind stresses. Outside of Poverty Bay, currents were on average to the southwest (Fig. 7d), and while some material was transported to the north of Poverty Bay, delivery was primarily to the southwest. During this eleven-day event, areas shallower than ~20 m in Poverty Bay and the coast to the north of Poverty Gap experienced net erosion, and the model increased the amount of riverine sediment on the shelf by 40–100%, depending on settling velocity, with net deposition focused at the bay mouth and to either side of Poverty Bay (Fig. 7c).

Though less effective at transporting sediment than the August 31 storm, a series of five smaller river discharge and wave events redistributed and added to the flood deposit during this two-month winter period. The discharges together delivered 2×10^9 kg of riverine sediment, about ~1/4 of the July 6 flood load. Fluxes were predominantly to the south-southwest. The model produced net deposition in deeper areas of Poverty Bay, on the inner- and mid-shelf (up to 55 m deep) to the south of Poverty Bay due to southwestward currents, and on the mid-shelf (30–55 m deep) to the north of Poverty Bay (Fig. 7e and f). Net erosion occurred in shallow areas of Poverty Bay, Poverty Gap, and the coast north of the river mouth.

4.2. Hydrodynamic climate and sedimentation during the 2010 field season

Whereas Section 4.1 analyzed model results for specific events, this section examines calculations for the entire thirteen-month model run to gain insight into the cumulative effects of multiple transport events superimposed on background conditions, and the relative importance of the large magnitude episodes of transport within the longer time frame.

4.2.1. Waves

Waves dominated bed stresses across the shelf, and therefore wave properties determined the frequency and magnitude of sediment resuspension, and impacted how resuspension varied with water depth. Waves traveled from the southeast onto the shelf, and had an average height and period of 1.5 m and 8.2 s, estimated by the New Zealand wave model used as model input (Tolman et al., 2002, implementation described in Moriarty et al., 2014). The resulting wave-induced bed shear stresses exceeded those induced by currents by an order of magnitude (Fig. 8b and c), and therefore dominated the resuspension of sediment, so that the occurrence of energetic waves determined the timing of resuspension events. To evaluate the frequency of wave-induced resuspension (Fig. 8a), we assumed that conditions where bed stress exceeded 0.15 Pa were energetic enough to suspended sediment. Bed shear stresses exceeded this threshold 94%, 52%, and 26% of the time at water depths of 20, 40, and 60 m, respectively. Even during relatively modest conditions when wave height was ~1.5 m, bed stresses exceeded the 0.15 Pa threshold across the shelf, depending on wave period. Thus, although bed stresses and resuspension were reduced in deeper regions, conditions were frequently energetic enough to rework riverine deposits over the entire continental shelf (Figs. 2, 8 and 9).

4.2.2. Currents

Currents naturally influenced suspended sediment flux magnitude and direction, and therefore affected sediment budgets (Figs. 4–7 and 10). Water velocities were usually oriented along isobaths, but switched direction often, as did observed currents from tripod deployments (Fig. 2d and e). On average, water velocities in much of the model domain were directed toward the north–northeast (about 60% of the time), and the largest fluxes of water were in that direction (Fig. 10). The time-averaged current

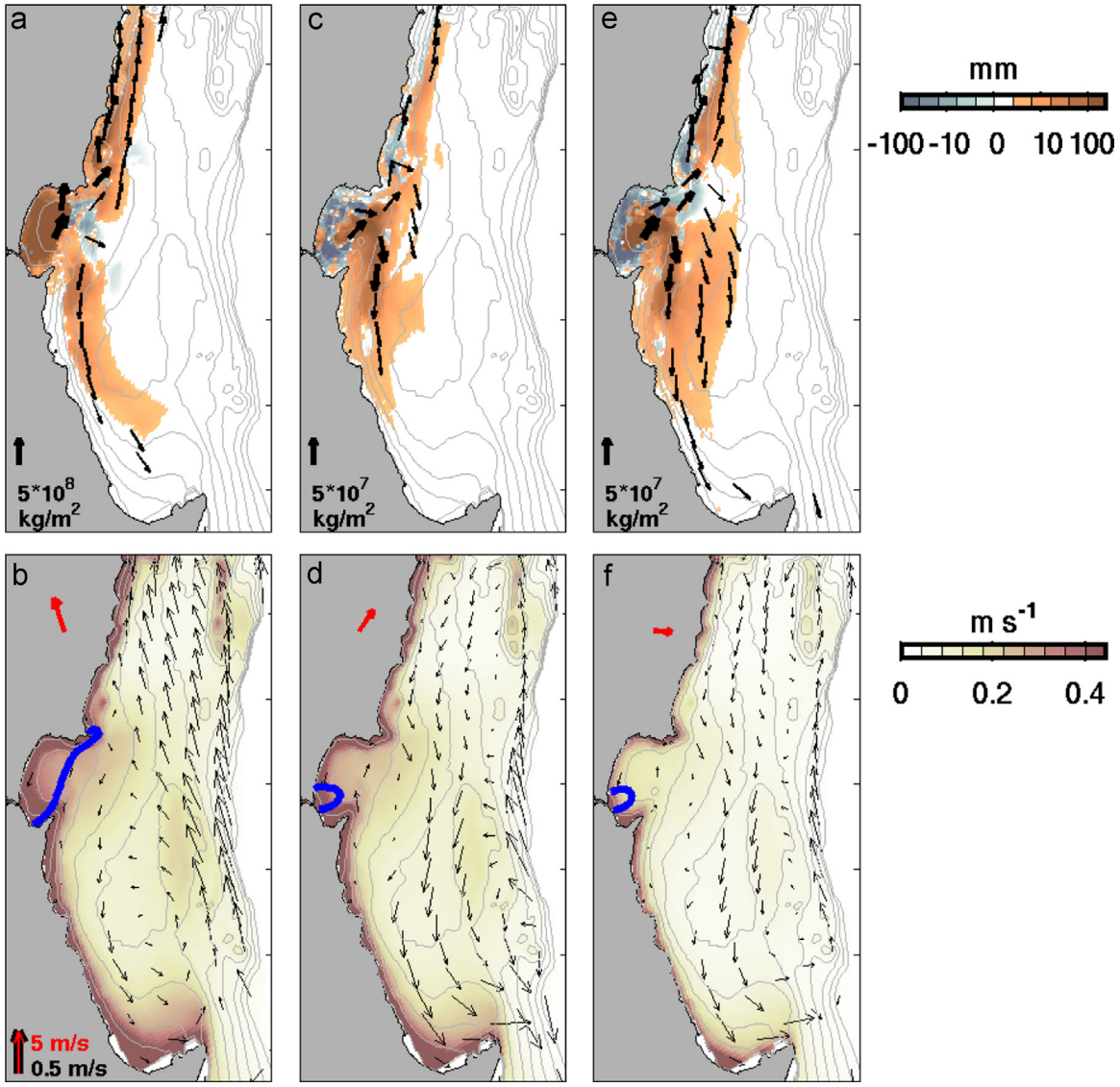

Fig. 7. Same as Fig. 5, but for time periods during and following the July flood, including flood conditions (a) and (b) July 4-22, 2010; an energetic wave event (c) and (d) August 29 – September 8, 2010; and months of moderate waves and discharges: (e) and (f) July 22 – September 30, 2010.

velocities showed a lot of spatial variability, including a counter-clockwise eddy that often formed landward of the Lachlan anticline between the bay mouth and Mahia Peninsula (Fig. 10b). This feature acted to retain sediment south of Poverty Gap in the vicinity of the southern depocenter.

4.2.3. Sediment fluxes and accumulation

Sediment fluxes, determined by currents and suspended sediment concentrations, influenced the location of riverine deposits by directing material either north or south of the bay mouth and by impacting the relative amounts of sediment retained in the bay versus delivered to the shelf. Fluxes of riverine material in Poverty Bay were primarily directed towards the bay mouth and were dominated by transport during floods within the freshwater plume and the bottom boundary layer. Outside of Poverty Bay, the direction of sediment fluxes depended on shelf currents, e.g. see Figs. 4–6 and 10. Although net transport, i.e. spatially- and temporally averaged fluxes, on the shelf were directed northward (Fig. 10), currents at the mouth of Poverty Bay and in Poverty Gap varied in direction. At the bay mouth, transport diverged, with net sediment fluxes oriented toward the northeast and southwest on each side of the bay mouth (Fig. 10). Northeastward fluxes were dominated by river plume transport, whereas southwestward fluxes occurred due to combinations of near-bed currents, southwestward shelf currents, and a persistent eddy south of the bay mouth. Indeed, ongoing work suggests that the near-bed fluxes were gravity-driven in some areas of the shelf during periods of energetic waves and high suspended sediment concentrations. Such areas included the mouth of Poverty Bay and, consistent Hale et al.'s, (2014a) observations, in Poverty Gap. Farther offshore, at the 40 m isobath in Poverty Gap, along-shelf currents and sediment fluxes were primarily directed along-shore, with about equal amounts of sediment being transported northeast and southwestward due to the oscillating currents (Fig. 11). Over the thirteen-month model run, these along-shelf suspended fluxes negated each other, so the net sediment flux at Poverty Gap was offshore (Figs. 10 and 11).

Overall, the largest sediment fluxes within the model domain occurred during floods and wave events. The three floods during the 2010 field season (in January, July, and October), and the largest wave events after each flood (in March, August, and October), accounted for about 61% and 14% of fluxes, respectively. Overall, suspended fluxes during floods exceeded those in low energy conditions by about two orders of magnitude, and exceeded fluxes

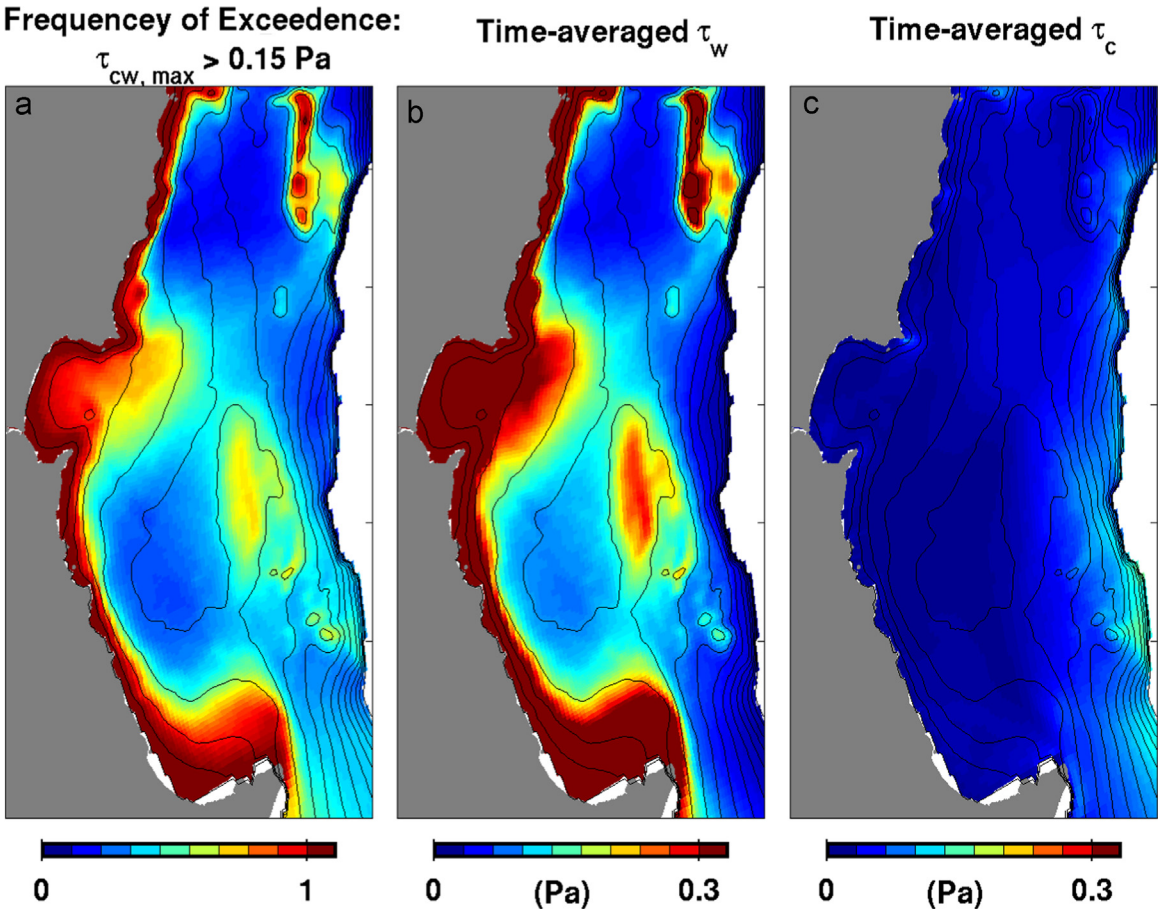

Fig. 8. (a) Percent of the time that wave- and current- induced bed shear stresses exceeded 0.1 Pa., (b) average wave-induced bed shear stress (Pa), and (c) average current-induced bed shear stress (Pa) from January 15, 2010 to February 15, 2011.

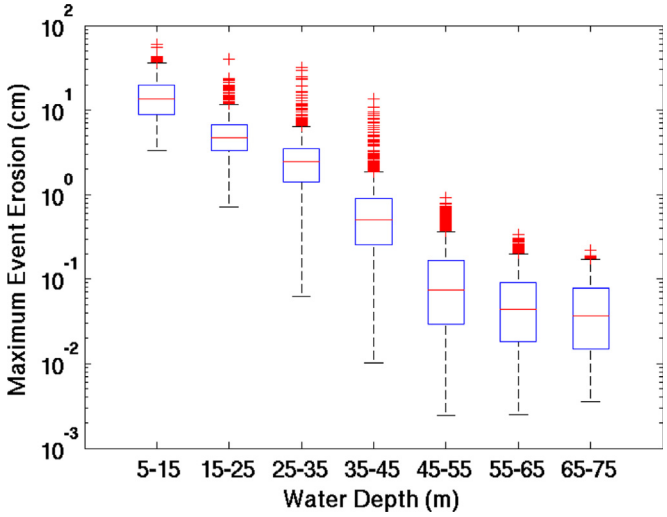

Fig. 9. Maximum net erosion observed at each grid cell within any 10 day period during the model run, binned by water depth, from January 15, 2010–February 15, 2011. For each bin, the 25% and 75% quartiles are shown by the blue box; the median is shown by the red line; and the black lines indicate the range of the model estimates, i.e. the 0% and 100% percentiles, excluding outliers, which are indicated with red crosses (For interpretation of the references to color in this figure legend, the reader is referred to the web version of this article).

during large wave events by one order of magnitude. Fluxes across the shelf were highest when both currents and waves were energetic; e.g., the faster velocities and increased resuspension caused shelf sediment fluxes to more than double during the July flood compared to the January flood, consistent with tripod observations (Hale et al., 2014a). Excluding floods, the highest suspended sediment fluxes occurred during larger and more sustained wave events when bed stresses remained elevated, e.g. exceeding 1 Pa at 40 m depth, for at least a few days (Fig. 2). The model also estimated that fluxes were elevated for resuspension events following high discharges because of the increased sediment availability. For example, calculated sediment fluxes were about five times higher during the moderate wave event on 2/18/2010 compared to those on 4/21/2010 because that event occurred soon after a discharge pulse, even though bed stresses during the first event were only about half as strong.

Although sedimentation patterns varied on timescales of days to months (see Section 4.1, Fig. 11), net accumulation over the entire thirteen-month model run occurred in Poverty Bay and on the shelf to either side of Poverty Gap between 30 and 55 m water depth (Fig. 10). Deposition was reduced in Poverty Gap where shallow water depths increased wave-induced bed stresses and resuspension (Figs. 8–10). Settling velocity strongly influenced modeled sediment budgets (Table 2; see Section 5.1) and depositional footprints (i.e. shape of the deposit) (Fig. 3). The longer residence time of slower-settling sediment in the water column during floods and resuspension events increased its dispersal relative to faster settling material (Fig. 3). By the end of the thirteen-month model run, distinct dispersal patterns were estimated for the different classes of sediment on the continental shelf (Fig. 3e–h). The model distributed slower-settling sediment (w_s=0.15 mm/s) on the shelf to either side of Poverty Gap, with thinner deposits on Poverty Gap. In contrast, sediment settling at 1 mm/s formed a

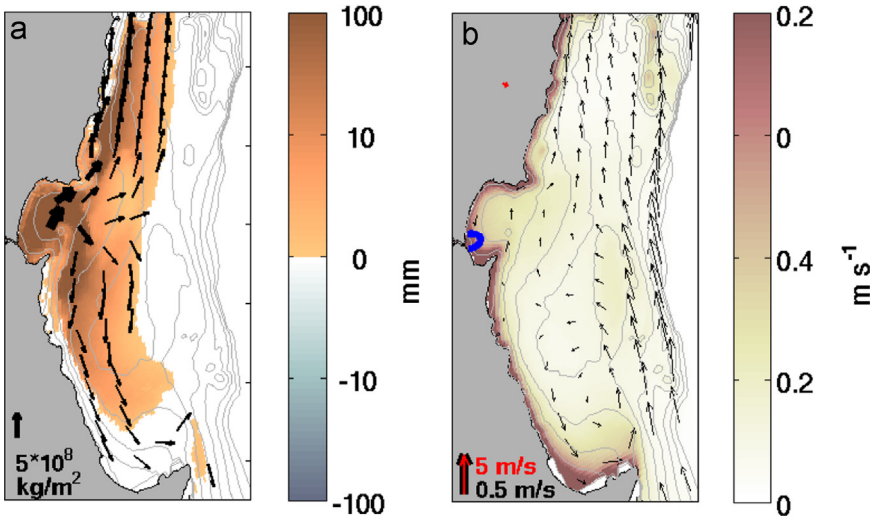

Fig. 10. Cumulative sediment fluxes and hydrodynamic conditions integrated from January 15 2010–February 15, 2011; similar to Figs. 5 and 7, but covering the entire model run. (a) Cumulative deposition (positive) and erosion (negative) of riverine sediments, shown when changes in seabed height exceed 1 mm. Flux arrows shown for every 10 grid cells where fluxes exceed 2×10^6 kg m^2, except as noted. (b) Time-averaged wave orbital velocities (shading), depth-averaged currents (black arrows), surface salinity (blue contour representing 32 ppt), and spatially-averaged wind (red arrow). Currents shown for every 12 grid cells (For interpretation of the references to color in this figure legend,the reader is referred to the web version of this article).

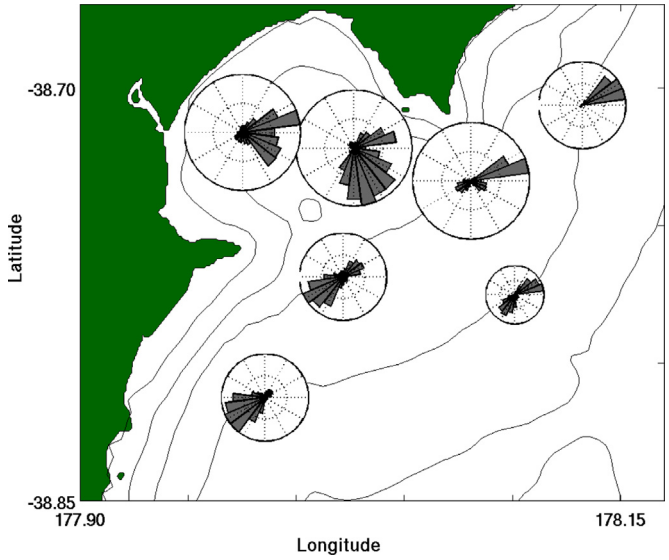

Fig. 11. Rose diagrams of time-integrated flux magnitude (kg m^{-1}) during the model run, from January 15, 2010–February 15, 2011. Small, medium, and large diagrams indicate locations with maximum binned values of less than 10^5,10^5–10^6, and over 10^6 kg m^{-1}.

narrower, shallower deposit at the mouth of Poverty Bay that crossed Poverty Gap with preferential deposition to the northeast.

5. Discussion

This section discusses factors that may explain differences between observed and modeled deposition and sediment budgets (Section 5.1), synthesizes results in the context of Wright and Nittrouer's (1995) dispersal stages of riverine sediment dispersal (Section 5.2), discusses the formation and possible preservation of event layers at the study site (Section 5.3), and compares the Waipaoa to other shelves (Section 5.4).

5.1. Evaluation of sedimentation estimates and modeling limitations

Our previous analysis (Moriarty et al., 2014) found that model estimates captured several features observed for the Waipaoa, including the episodic timing of sediment delivery during floods, dispersal of material to both sides of Poverty Bay, reworking by wave events, and the resulting spatial and temporal variability in deposition. This section focuses on event sedimentation and export of material from Poverty Bay to the shelf, which were not discussed in Moriarty et al. (2014), and then on factors affecting model representation of these two processes. Throughout the section, we evaluated the modeled patterns of erosion and deposition using measured ^{7}Be inventories reported by Walsh et al. (2014) and Kniskern et al. (2014).

Overall, model-estimated deposits generally occurred in shallower water than the locations of observed high ^{7}Be inventories, and the model seemed to over-estimate accumulation in Poverty Bay (Figs. 3, 5 and 10; Kniskern et al., 2014; Walsh et al., 2014). Whereas earlier observations have shown that floods ephemerally deposit sediment within Poverty Bay (Bever et al., 2011), only a handful of the sediment cores from Walsh et al. (2014) or Kniskern et al. (2014) evaluated deposition within Poverty Bay during the modeled time period. Therefore, the observationally–based methods were unable to quantify the role of Poverty Bay in event-scale sediment budgets. Nonetheless, we suspect the model retains more sediment within the bay than actually occurs.

An event timescale analysis of deposition shortly after the January flood indicated that riverine sedimentation extended from the northern depocenter, across Poverty Gap near the 30–50 m isobaths, to parts of the southern depocenter (Kniskern et al., 2014). Model estimates, especially for slower-settling material, captured aspects of this sedimentation, including high deposition in Poverty Gap up to ~45 m water depth and to either side of Poverty Bay (Figs. 3 and 5). Estimated sedimentation near the Southern depocenter was less than 1 mm thick, however, whereas ^{7}Be was observed there in sediment layers as deep as 8 cm (Kniskern et al., 2014). Factors including wave resuspension and bioturbation (Section 5.3), seabed consolidation (see Moriarty et al., 2014), high spatial variability of shelf depositional patterns (Walsh et al., 2014; Kniskern et al., 2014; e.g. Fig. 4), the underestimation of across shelf sediment fluxes, and uncertainties in sediment properties, discussed below, help explain these discrepancies.

Modeled across-shelf sediment fluxes were likely

underestimated, as overall suspended fluxes were low, and near-bed gravity flows were neglected. As Moriarty et al. (2014) noted, modeled bed stresses captured the timing of wave events, but estimated suspended sediment concentrations and across-shelf currents consistently fell below values derived from tripod observations. This implies that model estimates of across-shelf flux underestimated the true values. Also, while our model accounted for gravity-driven transport, it lacked sufficient vertical resolution to represent thin near-bed gravity flows observed on the Waipaoa during some wet storms (Hale et al., 2014b) and other shelves (e.g. Traykovski et al., 2000; Ma et al., 2008). These gravity flows seem more capable of creating thick event beds than dilute suspensions (Harris et al., 2005), and can transport sediment further offshore (Ma et al., 2008). To complement Hale et al.'s (2014a, 2014b)point observations of gravity-driven transport during the July flood and one-dimensional model, and Bever (2014)and Harris' modeling of gravity-driven transport in Poverty Bay, future efforts may more thoroughly investigate the role of gravitational forcing on Waipaoa's shelf depositional patterns, perhaps using a higher-resolution ROMS model, or a gravity flow model similar to Ma et al. (2010) and Scully et al. (2003).

Finally, as noted in the results, modeled sediment fluxes and budgets depended strongly on the assumed settling velocities for each sediment class (Fig. 3, Table 2). Although little material from any of the sediment classes was deposited deeper than ~50 m water depth during the model run, uncertainties in settling velocity would affect the across-shelf export of material.

5.2. Links between event timescale processes and depositional patterns

This section analyzes sediment dispersal by comparing results from different events and considering timescales that range from days to thirteen months, based on Wright and Nittrouer's (1995) classification of the four stages of riverine sediment dispersal. Overall, although initial sedimentation during floods varied depending on the currents, wave processes encouraged the movement of material from initial deposits towards longer-term shelf depocenters. In other words, Dispersal Stages I and II delivered material to the shelf with deposition varying widely between events in response to larger-scale current, wind, and wave patterns. The accumulation of sediment over timescales of years and longer (Dispersal Stage IV), however, was controlled by the redistribution of sediment during episodic wave events (Dispersal Stage III), with accumulation highest in areas where wave bed stresses reach local minima (Figs. 1a and 8).

5.2.1. Delivery of sediment via river plumes

Delivery of sediment via the river plume constitutes Stage I of Wright and Nittrouer's (1995) conceptual model of continental margin sedimentation. On the Waipaoa shelf, periods of elevated discharge accounted for nearly all (99.5%) of the fluvial sediment input to the coastal ocean. Variations in winds and hydrodynamic forcing influenced transport of this material within freshwater plumes, as described below.

The two large floods that occurred in January and July of our study exhibited similar phases to those noted in Orpin et al. (2006) and Bever et al. (2011). That is, for both floods, delivery of sediment via the riverplume included an initial phase when strong shoreward winds retained the plume and associated material within or to the south of Poverty Bay, then passage of the storm caused winds to weaken as they rotated to blow seaward. During the falling limb of the hydrograph, winds at times blew strongly seaward, which helped to flush freshwater and suspended sediment to the continental shelf. Once on the shelf, the wind-forced currents were also impacted by the strength and direction of larger-scale continental shelf currents. Differences in the floods' behavior during Dispersal Stage I were related to the relative strengths of the wind-forced and large-scale currents during the later phases of the flood event (e.g. Figs. 4 and 6). The northeastward tendancies of both the larger-scale currents and winds during the July flood encouraged formation of a narrow, “downwelling-type” plume that stayed close to shore and generally remained shoreward of the 30 m isobath. In contrast, a southwestward larger-scale current that was enhanced by predominantly shoreward local winds during the January flood resulted in a wider “upwelling-type” plume that at times extended past the 50 m isobath, but remained on the proximal shelf.

5.2.2. Initial flood sedimentation

Initial flood deposition constitutes Dispersal Stage II of Wright and Nittrouer's (1995) conceptual model. Overall, although the winds followed a similar pattern in both the January and July floods, their initial depositional patterns varied signficantly in response to differences in shelf currents and wave energy (Figs. 5 and 7). For instance, during the January flood, relatively low wave energy encouraged deposition near the river mouth. Additionally, the river plume dispersed sediment broadly, causing a radially-shaped depositional footprint. Conversely, for the July flood, energetic waves, southward near-bed fluxes, and the presence of an eddy over the southern depocenter encouraged deposition to occur along the coast, southwest of Poverty Bay.

5.2.3. Reworking of initial flood deposits

Wright and Nittrouer (1995) define Dispersal Stage III as a period of post-depositional reworking of riverine deposits. In the context of the Waipaoa shelf, Stage III reworking occurred in the weeks to months following floods, when initial deposits were episodically resuspended during periods of energetic waves, and redistributed across and along the shelf, consistent with other studies on this margin (Bever et al., 2011, Bever and Harris, 2014, Hale et al., 2014a). The model calculations presented here highlight the importance of Stage III for the Waipaoa shelf, as discussed below.

Although energetic waves triggered these episodes of reworking, the magnitude and direction of sediment fluxes varied depending on the strength and direction of shelf currents (e.g. Figs. 5 and 7). Comparing calculations for the two large wave events (March 7 and August 31) highlights the sensitivity of Dispersal Stage III sediment reworking to these currents. During both times, wave heights exceeded 3.5 m. During the March event, northward currents driven by larger scale flow and winds were particularly effective at transporting sediment alongshore, consistent with tripod observations in Poverty Gap (Hale et al., 2014a). In contrast, slower currents during the peak of the August 31 wave event were directed westward, and so fluxes were smaller and less sediment was removed from Poverty Bay and the shelf. These differences in shelf currents during periods of reworking (Dispersal Stage III), as well as during the floods (Dispersal Stages I and II), can explain the variability in modeled deposition patterns and the ^{7}Be signatures observed on the shelf.

Although patterns of sediment flux varied during Dispersal Stage III, wave resuspension encouraged net fluxes of material from shallow to deeper areas. Bathymetry exerted strong controls on wave orbital velocities, so that bed stresses in Poverty Bay, in Poverty Gap and on the anticlines surpassed those in the long-term depocenters (Fig. 8b). Because bed stresses were higher in shallower areas, sediment was preferentially resuspended there (Fig. 9), and so resuspension by energetic waves encouraged retention of material in the relatively deep depocenters located on either side of Poverty Gap (Fig. 10). Dry wave events especially reinforced this pattern because they did not coincide with the

input of new riverine sediment (Fig. 5). In contrast, drapes of newly-delivered material often settled over Poverty Gap during wet wave events, obscuring the gap between the two distinct depocenters (Fig. 7). Thus, although patterns of sediment flux varied during Dispersal Stage III on timescales of days to weeks (Figs. 4–7 and 11), often changing the riverine 'footprint', wave events were essential for delivering sediment from the bay and Poverty Gap to deeper areas of the shelf.

5.2.4. Sediment accumulation

Dispersal Stage IV of Wright and Nittrouer (1995) represents the accumulation of material in depocenters over decadal or longer timescales. Although our model only covers a thirteen-month period, the response of wave processes to the Waipaoa shelf bathymetry (Dispersal Stage III), described above, helps to explain the presence of two distinct shelf depocenters for terrestrial material, and the reduced accumulation in Poverty Gap that has been seen based on ^{210}Pb data for timescales of about a century (Miller and Kuehl, 2010). In fact, the total bed stress averaged over the thirteen-month model run showed similar spatial patterns to the long-term accumulation rates of Miller and Kuehl (2010), in that locations of high accumulation were associated with areas of minimal average bed stress (Figs. 1a and 8a). Because the wave component dominates bed stress on the Waipaoa shelf (Fig. 8b and c), the spatial patterns in bed stress are controlled by the shelf's bathymetry, particularly the two synclinal basins that have flanked Poverty Gap throughout the Holocene (Gerber et al., 2010). Therefore, despite the difference in timescales between our thirteen-month model run and century-scale (~100 years) accumulation rates from ^{210}Pb, the attenuation of wave stresses with water depth appears to facilitate long-term accumulation in these synclinal depocenters.

5.3. Formation and preservation of event layers

Model results can help with interpretations of riverine deposits and event layers which, on the Waipaoa shelf, were complicated by high spatial and temporal variability and, at times, by seemingly conflicting data. For instance, after the January 31, 2010 flood, only millimeters of net deposition were apparent from the altimeter measurements (Hale et al., 2014a) and the numerical model estimates, but measurable ^{7}Be activities were seen as deep as ~8 cm into the seabed two weeks after the event (Kniskern et al., 2014). While bioturbation may mix geochronological tracers vertically within the seabed (e.g. Bentley and Nittrouer, 2003; Lecroart et al., 2010), resuspension may also contribute to vertical mixing of fresh terrestrial sediment, especially during times of energetic waves. The model indicated that centimeters of sediment could be reworked by resuspension during a single wave event at 40 m water depth (Fig. 9). An older seabed layer capped by a thin flood deposit could therefore be resuspended and redeposited as a relatively thick layer containing fresh riverine material which would mix terrestrial markers, e.g. ^{7}Be, much deeper into the seabed than the initial flood deposit, even if the wave event caused minimal net deposition.

This study's results can also help interpret the observed seabed facies, which grade from physically to biologically dominated with distance from the river mouth (Rose and Kuehl, 2010). Increased sediment availability near the river mouth, and the relatively high bed stresses in shallow areas enhanced resuspension there which would produce physical laminations in the sediment (Figs. 8–10). Farther away from the river mouth, resuspension occurs less frequently and sediment concentrations are lower, so seabed facies are biologically dominated. Although changes in the benthic community and associated seabed characteristics on shelves can be driven by gradients in nutrients (e.g. Rhoads et al., 1985), the lack of spatial variability in salinity structure (model estimates, and unpublished CTD casts) likely limited strong spatial gradients in nutrient delivery offshore the Waipaoa River, except during floods or to areas within a kilometer of the river mouth. Therefore, variations in ephemeral deposition and near-bed turbidity, due to fluvial supply and resuspension frequency, likely drive the transition of seabed facies from physically- to biologically- dominated.

5.4. Transport on the Waipaoa margin compared to other small mountainous river systems

We compared our findings for the Waipaoa continental shelf to those from other recently studied small mountainous river systems such as the Eel River, USA and other rivers on that coast; Choshui (or Jhuoshuei) and Gaoping Rivers, Taiwan; Tet River, France; Besos River, Spain; rivers draining into the Adriatic Sea; and the Waiapu River, New Zealand. This discussion focuses on the generality of our findings that rotating winds during storms influence flood sedimentation (Dispersal Stages I and II); that depositional patterns on timescales of days to weeks vary due to larger-scale currents (Dispersal Stage III); and that, despite short-term variability, the net result of Dispersal Stage III reworking is accumulation of material in deeper areas of the shelf (Dispersal Stages III and IV).

Plume behavior and sediment deposition during floods (Dispersal Stages I and II) on the Waipaoa shelf were sensitive to wind forcing. Waipaoa winds are variable in direction, and blow from the northeast, the most common wind direction, less than a quarter of the time during floods (based on wind records from Gisborne airport from 1967 to 2002 from Kniskern, pers. comm., 2015; Kniskern et al., 2014). Within individual floods, rotating winds on the Waipaoa changed the direction of the river plume during the different phases of the flood. While this behavior is similar to that seen on the Waiapu margin located about 120 km to the northeast (Kniskern, 2007), winds on some other margins tend to be less variable during floods. On the Eel shelf, for example, south winds dominate during flood conditions (Sommerfield and Nittrouer, 1999; Kniskern et al., 2011), enhancing the Coriolis-driven tendency so that the Eel plume most often flows northward (Geyer et al., 2000). Differences in flood sedimentation (Dispersal Stage II) on these three margins are consistent with differences in river plume behavior and wind patterns (Dispersal Stage I), with the Eel plume usually delivering material north of the river mouth whereas the Waipaoa and Waiapu plumes disperse sediment in more radial patterns.

In addition to winds, larger-scale currents played an especially important role on the Waipaoa on timescales of days to weeks (Dispersal Stages I–III), especially during periods of reworking (Dispersal Stage III). Similar to other margins, both wet and dry floods redistributed riverine deposits in the days to months following initial emplacement. On most of these margins, however, larger-scale currents and/or gravity flows tend to move material in a consistent direction. Currents typically transport resuspended sediments southward along the coast offshore the Tet River (Guillen et al., 2006) and Besos River (Grifoil et al., 2014) in the western Mediterranean, and northward offshore the Choshui River in the Taiwan Strait (Liu et al., 2008), for example. Similarly, gravitational fluxes are always downslope, i.e. usually seaward, and have appeared to significantly impact sediment fluxes during Dispersal Stage II and III on the Waiapu shelf (Kniskern, 2007; Ma et al., 2008) and the Eel Shelf (Traykovski et al., 2000; Harris et al., 2005). In contrast, larger-scale currents on the Waipaoa shelf oscillate frequently, carrying suspended sediment back and forth along the shelf, so that modeled and observed sedimentation patterns varied among individual wave events over timescales of days to weeks (Figs. 5, 7 and 11; Walsh et al., 2014; Hale et al., 2014a).

Despite the short-term variability in sedimentation during Dispersal Stages I–III, over time the net result of Dispersal Stage III and IV reworking on the Waipaoa Shelf is delivery and

accumulation of riverine material in the relatively deeper areas of the shelf. This is similar to other margins, although delivery to Waipaoa depocenters did not coincide with floods. For some other small mountainous rivers, delivery to shelf or offshore depocenters primarily occurs during floods that often coincide with energetic oceanic conditions (e.g. Eel: Traykovski et al., 2000; Harris et al., 2005; Gaoping: Selvaraj et al., 2015). Transport on the Waipaoa and some other shelves differs from this model because transport to depocenters occurs in a series of 'steps' during episodic wave events following initial emplacement. In the Mediterranean Sea, for example, deposition near the Tet River mouth, delivered in the waning portion of a flood, was only exported to deeper areas during subsequent wave events (Guillen et al., 2006). This decoupling of Dispersal Stages I and II from III and IV is especially important for sites such as the Waipaoa shelf, where energetic waves occur throughout the year, in contrast to margins where wave energy is more seasonal and peaks during flood season (e.g. US west coast: Kniskern et al., 2011). This decouping encourages the near-continuous reworking of flood deposits in shallow areas and emphasizes the importance of Dispersal Stage III for sediment dispersal on the Waipaoa shelf.

6. Conclusions

This paper analyzed results from a hydrodynamic-sediment transport model to evaluate sediment dispersal and deposition throughout a thirteen-month study period over event to seasonal timescales on the continental shelf offshore the small mountainous Waipaoa River. On timescales of hours to days, hydrodynamic conditions fluctuated due to oscillations in larger-scale currents and shifts in winds. These changing conditions caused the riverine depositional footprints to vary greatly over short timescales (Figs. 4–7), which is consistent with ^{7}Be observations showing different patterns of recent terrestrial deposition on each research cruise during this time period (Walsh et al., 2014; Kniskern et al., 2014). Overall, sedimentation patterns varied among the phases of individual floods; and differed for the two large floods considered here, and among individual wave events. This highlights the Waipaoa Sedimentary System's sensitivity to hydrodynamic forcing on the continental shelf during event-timescales.

Despite the variability of sedimentation on short timescales, wave-induced bed stress patterns were related to the longer-term depositional patterns seen in geochronological records of ^{210}Pb. Because wave energy and bed stress attenuate with water depth, deeper areas of the shelf were relatively protected from wave-dominated resuspension. This led to preferential erosion of deposits from shallower locations and encouraged accumulation in deeper water where bed stresses were lower (Figs. 8–10). In this manner, shelf bathymetry and modern event-timescale bed stresses (Fig. 8) help to explain the presence of long-term depocenters in bathymetric lows that lie to either side of Poverty Gap.

Overall, this study demonstrates the importance of the reworking of initial flood deposits, i.e. Wright and Nittrouer's (1995) Dispersal Stage III, for the dispersal of material from the Waipaoa River. Offshore of some small mountainous rivers, e.g. the Eel River, USA (Traykovski et al., 2000; Harris et al., 2005) and the Gaoping River, Taiwan (Selvaraj et al., 2015), material is transported rapidly during floods to areas serving as loci of long-term deposition, consistent with Wright and Nittrouer's (1995) assertion that initial deposition (Dispersal Stage II) is especially important for small mountainous rivers. However, on the Waipaoa margin, transport to the final location of deposition seemed to occur in multiple steps that included both the initial flood and subsequent wave-driven resuspension events. This implies that oceanographic transport mechanisms provide especially important controls on depositional patterns there. That is, shelf deposition depended strongly on oceanographic transport (waves and currents), in addition to source characteristics such as flood size and sediment size distribution.

Acknowledgments

Funding was provided by NSF MARGINS Grant OCE- (Moriarty and Harris), a VIMS institutional student fellowship (Moriarty), and NIWA as part of its government-funded core research (Hadfield). Datasets useful during the development and testing of the model were provided by personnel from NIWA (M. Uddstrom, S. Stephens, A. Orpin), VIMS (S. Kuehl, T. Kniskern), the USACoE (J. McNinch), GDC (G. Hall, D. Peacock), ECU (J.P. Walsh, R. Corbett, J. Kiker), and UW (A. Ogston, R. Hale). Thank you to A. Bever (now at Anchor QEA), A. Miller, M.A. Bynum, D. Weiss, T. Crockett (all from VIMS/William & Mary), and A. Kettner (University of Colorado; UC). Computational facilities at VIMS, the SciClone cluster at the College of William & Mary, and the CSDMS computing cluster at UC were supported by NSF, VA Port Authority, Sun Microsystems, and Virginia's Commonwealth Technology Research Fund. High-performance computing facilities at NIWA were supported by the NZ eScience Infrastructure (NESI) and funded by NESI's collaborator institutions and through the Ministry of Business, Innovation & Employment's Research Infrastructure programme. Comments from C. Friedrichs, S. Kuehl, and L. Schaffner (all at VIMS), two anonymous reviewers, and CSR Editor R. Sternberg benefitted the manuscript's development. This is contribution 3506 of the Virginia Institute of Marine Science.

References

Ariathurai, C.R., Arulanandan, K., 1978. Erosion rates of cohesive soils. J. Hydraul. Div. 104 (2), 279–282.
Bentley, S.J., Nittrouer, C.A., 2003. Emplacement, modification, and preservation of event strata on a flood-dominated continental shelf: Eel shelf, Northern California. Cont. Shelf Res. 23, 1465–1493.
Bever, A.J., 2010. Integrating Space– and Time-scales of Sediment-transport for Poverty Bay, New Zealand (Ph.D. dissertation). College of William & Mary, Williamsburg, VA.
Bever, A.J., Harris, C.K., McNinch, J.E., 2011. Hydrodynamics and sediment-transport in the nearshore of Poverty Bay, New Zealand: observations of nearshore sediment segregation and oceanic storms. Cont. Shelf Res. 31, 507–526.
Bever, A.J., Harris, C.K., 2014. Storm and fair-weather driven sediment-transport within Poverty Bay, New Zealand, evaluated using coupled numerical models. Cont. Shelf Res. 86, 34–51.
Blair, N.E., Leithold, E.L., Aller, R.C., 2004. From bedrock to burial: the evolution of particulate organic carbon across coupled watershed-continental margin systems. Mar. Chem. 92, 141–156.
Brackley, H.L., Blair, N.E., Trustrum, N.A., Carter, L., Leithold, E.L., Canuel, E.A., et al., 2010. Dispersal and transformation of organic carbon across an episodic, high sediment discharge continental margin, Waipaoa sedimentary system, New Zealand. Mar. Geol. 270 (1–4), 202–212.
Carter, L., Orpin, A.R., Kuehl, S.A., 2010. From mountain source to ocean sink – the passage of sediment across an active margin, Waipaoa sedimentary system, New Zealand. Mar. Geol. 270 (1–4), 1–10.
Chiswell, S.M., 2000. The Wairarapa coastal current. N. Z. J. Mar. Freshw. Res. 34 (2), 303–315.
Chiswell, S.M., 2005. Mean and variability in the Wairarapa and Hikurangi eddies, New Zealand. N. Z. J. Mar. Freshw. Res. 39 (1), 121–134.
Chiswell, S.M., Roemmich, D., 1998. The east cape current and two eddies: a mechanism for larval retention? New. Zealand J. Mar. Freshw. Res. 32 (2), 385–397.
Foster, G., Carter, L., 1997. Mud sedimentation on the continental shelf at an accretionary margin—Poverty Bay New Zealand. N. Z. J. Geol. Geophys. 40, 157–173.
Gerber, T.P., Pratson, L.F., Kuehl, S., Walsh, J.P., Alexander, C., Palmer, A., 2010. The influence of sea level and tectonics on late Pleistocene through Holocene sediment storage along the high-sediment supply Waipaoa continental shelf. Mar. Geol. 270 (1–4), 139–159.
Geyer, W.R., Hill, P., Milligan, T., Traykovski, P., 2000. The structure of the Eel River plume during floods. Cont. Shelf Res. 20, 2067–2093.
Gomez, B., Carter, L., Trustrum, N.A., Palmer, A.S., Roberts, A.P., 2004. El Niño–Southern oscillation signal associated with middle Holocene climate change in

intercorrelated terrestrial and marine sediment cores, north island, New Zealand. Geology 32 (8), 653–656.
Griffiths, G./A., Glasby, G.P., 1985. Input of river-derived sediment to the New Zealand continental shelf: I. Mass. Estuar. Coast., Shelf Sci. 21, 773–787.
Grifoil, M., Grada, V., Aretxabaleta, A., Guillen, J., Espino, M., Warner, J.C., 2014. Formation of fine sediment deposit from a flash flood river in the Mediterranean Sea. J. Geophys. Res. Oceans 1999 (5837), 5853.
Guillen, J., Bourrin, F., Palanques, A., Durrieu de Madron, X., Puig, P., Buscail, R., 2006. Sediment dynamics during wet and dry storm events on the Tet inner shelf (SW Gulf of Lions). Mar. Geol. 234, 129–142.
Hadfield, M.G., Rickard, G.J., Uddstrom, M.J., 2007. A hydrodynamic model for Chatham Rise, New Zealand. N. Z. J. Mar. Freshw. Res. 41 (2), 239–264.
Haidvogel, D.B., Arango, H.G., Hedstrom, K., Beckmann, A., Malanotte-Rizzoli, P., Shchepetkin, A.F., 2000. Model evaluation experiments in the North Atlantic basin: simulations in nonlinear terrain-following coordinates. Dyn. Atmos. Oceans 32 (3–4), 239–281.
Haidvogel, D.B., Arango, H., Budgell, W.P., Cornuelle, B.D., Curchitser, E., Di Lorenzo, E., et al., 2008. Ocean forecasting in terrain-following coordinates: formulation and skill assessment of the regional ocean modeling system. J. Comput. Phys. 227 (7), 3595–3624.
Hale, R., Ogston, A., Walsh, J.P., Orpin, A., 2014a. Sediment transport and event deposition on the Waipaoa River Shelf, New Zealand. Continental Shelf Research.
Hale, R. Ogston, A., Walsh, J.P., 2014b. In-situ observation of wave-supported fluid mud on the continental shelf. Ocean Sciences Biennial Meeting, Honolulu, Hawaii.
Harris, C.K., Traykovski, P., Geyer, W.R., 2005. Flood dispersal and deposition by near-bed gravitational sediment flows and oceanographic transport: a numerical modeling study of the eel river shelf, northern California. J. Geophys. Res. 110 (C09025).
Harris, C.K., Wiberg, P., 2002. Across-shelf sediment transport: interactions between suspended sediment and bed sediment. J. Geophys. Res. 107, 3008.
Hicks, D.M., Gomez, B., Trustrum, N.A., 2000. Erosion thresholds and suspended sediment yields, Waipaoa River basin, New Zealand. Water Resour. Res. 36 (4), 1129–1142.
Hicks, D.M., Gomez, B., Trustrum, N.A., 2004. Event suspended sediment characteristics and the generation of hyperpycnal plumes at river mouths: east coast continental margin, north island, New Zealand. J. Geol. 112 (4), 471–485.
Kiker, J.M., 2012. Spatial and Temporal Variability in Surficial Seabed Character, Waipaoa River Margin, New Zealand (M.S. thesis). East Carolina University, Greenville, NC.
Kniskern, T.A., 2015. Personal Communication.
Kniskern, T.A., 2007. Shelf Sediment Dispersal Mechanisms and Deposition on the Waiapu River Shelf, New Zealand (Ph. D. dissertation). College of William & Mary, Williamsburg, VA.
Kniskern, T.A., Mitra, S., Orpin, A.R., Harris, C.K., Walsh, J.P., Corbett, D.R., 2014. Characterization of a flood-associated deposit on the Waipaoa River shelf using radioisotopes and terrigenous organic matter abundance and composition. Cont. Shelf Res. 86, 66–84.
Kniskern, T.A., Warrick, J.A., Farnsworth, K.L., Wheatcroft, R.A., Goni, M.A., 2011. Coherence of river and ocean conditions along the US West Coast during storms. Cont. Shelf Res. 31, 789–805.
Kuehl, S.A., Alexander, C.A., Blair, N.E., Harris, C.K., Marsaglia, K.M., Ogston, A.S., Orpin, A.R., Roering, J.J., Bever, A.J., Bilderback, E.L., Carter, L., Cerovski-Darriau, C., Childress, L.B., Corbett, D.R., Hale, R.P., Leithold, E.L., Litchfield, N., Moriarty, J. M., Page, M.J., Pierce, L.E.R., Upton, P., Walsh, J.P., 2015. A source to sink perspective of the Waipaoa River margin. Earth Sci. Rev., In Press
Lecroart, P., Maire, O., Schmidt, S., Gremare, A., Anschutz, P., Meysman, F.J.R., 2010. Bioturbation, short-lived radioisotopes, and the tracer-dependence of biodiffusion coefficients. Geochim. Et. Cosmochim. Acta 74, 6049–6063.
Liu, J.P., Liu, C.S., Xu, K.H., Milliman, J.D., Chiu, J.K., Kao, S.J., Lin, S.W., 2008. Flux and fate of small mountainous rivers derived sediments into the Taiwan Strait. Mar. Geol. 256 (1), 65–76.
Ma, Y., Wright, L.D., Friedrichs, C.T., 2008. Observations of sediment transport on the continental shelf off the mouth of the Waiapu river New Zealand: evidence for current gravity flows. Cont. Shelf Res. 28 (4–5), 516–532.
Ma, Y., Friedrichs, C.T., Harris, C.K., Wright, L.D., 2010. Deposition by seasonal wave- and current-supported sediment gravity flows interacting with spatially varying bathymetry: Waiapu shelf, New Zealand. Mar. Geol. 275 (1–4), 199–211.
O.S. Madsen Spectral wave-current bottom boundary layer flows, In: Proceedings of the 24th International Conference on Coastal Engineering, ASCE, Kobe 1: pp. 384–398.
Miller, A.J., Kuehl, S.A., 2010. Shelf sedimentation on a tectonically active margin: a modern sediment budget for Poverty Continental Shelf, New Zealand. Mar. Geol. 270 (1–4), 175–187.
Milliman, J.D., Farnsworth, K.L., 2011. River Discharge to the Coastal Ocean: A Global Synthesis. Cambridge University Press, Cambridge.
Milliman, J.D., Syvitski, J.P.M., 1992. Geomorphic/tectonic control of sediment discharge to the ocean: the importance of small mountainous rivers. J. Geol. 100 (5), 525–544.
Moriarty, J.M., Harris, C.K., Hadfield, M.G., 2014. Implementation of a hydrodynamic and sediment transport model for the Waipaoa Shelf, New Zealand. J. Mar. Sci. Eng. 2 (2), 336–369.
Orpin, A.R., 2011. Personal Communication.
Orpin, A.R., Alexander, C., Carter, L., Kuehl, S., Walsh, J.P., 2006. Temporal and spatial complexity in post-glacial sedimentation on the tectonically active, Poverty Bay continental margin of New Zealand. Cont. Shelf Res. 26 (17–18), 2205–2224.
Orpin, A.R., Carter, L., Page, M.J., Cochran, U.A., Trustrum, N.A., Gomez, B., Palmer, A. S., Mildenhall, D.C., Rogers, K.M., Brackley, H.L., Northcote, L., 2010. Holocene sedimentary record from Lake Tutira: a template for upland watershed erosion proximal to the Waipaoa Sedimentary System, northeastern New Zealand. Mar. Geol. 270, 11–29.
Rhoads, D.C., Boesch, D.F., Zhican, T., Fengshan, X., Liqiang, H., Nilsen, K.J., 1985. Macrobenthos and sedimentary facies on the Changjiang delta platform and adjacent continental shelf, East China Sea. Cont. Shelf Res. 4 (1–2), 189–213.
Rose, L.E., 2012. Poverty Shelf, New Zealand from the Holocene to Present: Stratigraphic Development and Event Layer Preservation in Response to Sediment Supply, tectonics and climate (Ph.D. dissertation). College of William & Mary, Gloucester Point, VA.
Rose, L.E., Kuehl, S.A., 2010. Recent sedimentation patterns and facies distribution on the Poverty shelf, New Zealand. Mar. Geol. 270 (1–4), 160–174.
Sadler, P.M., 1981. Sediment accumulation rates and the completeness of stratigraphic sections. J. Geol. 89 (5), 569–584.
Scully, M.E., Friedrichs, C.T., Wright, L.D., 2003. Numerical modeling of gravity-driven sediment transport and deposition on an energetic continental shelf: Eel River, Northern California. J. Geophys. Res. 108, C4.
Selvaraj, K., Lee, T.Y., Yang, J.Y.T., Canuel, E.A., Huang, J.C., Dai, M., Liu, J.T., Kao, S.J., 2015. Stable isotopic and biomarker evidence of terrigenous organic matter export to the deep sea during tropical storms. Mar. Geol.
Shchepetkin, A.F., McWilliams, J.C., 2005. The regional oceanic modeling system (ROMS): a split-explicit, free-surface, topography-following-coordinate oceanic model. Ocean. Model. 9 (4), 347–404.
Shchepetkin, A.F., McWilliams, J.C., 2009. Correction and commentary for "Ocean forecasting in terrain-following coordinates: formulation and skill assessment of the regional ocean modeling system" by Haidvogel et al., J. comp. phys. 227, pp. 3595–3624. J. Comput. Phys. 228 (24), 8985–9000.
Smith, R.K., 1988. Poverty Bay, New Zealand: a case of coastal accretion. N. Z. J. Mar. Freshw. Res. 22 (1), 135–142.
Sommerfield, C.K., Nittrouer, C.A., 1999. Modern accumulation rates and a sediment budget for the Eel shelf: a flood-dominated depositional environment. Mar. Geol. 154, 227–241.
Stephens, S.A., Bell, R.G., Black, K.P., 2000. Complex circulation in a coastal embayment: Shelf-current, wind and density-driven circulation in Poverty Bay, New Zealand, In: Proceedings of International Coastal Symposium (ICS 2000): Challenges for the 21st Century in Coastal Science, Engineering and Environment, Rotorua, New Zealand, 34, pp. 45–59.
Tolman, H.L., Balasubramaniyan, B., Burroughs, L.D., Chalikov, D.V., Chao, Y.Y., Chen, H.S., Gerald, V.M., 2002. Development and implementation of wind-generated ocean surface wave modelsat NCEP*. Weather Forecast. 17, 311–333.
Traykovski, P., Geyer, W.R., Irish, J.D., Lynch, J.F., 2000. The role of wave-induced density-driven fluid mud flows for cross-shelf transport on the Eel River continental shelf. Cont. Shelf Res. 20, 2113–2140.
Walling, D.E., Webb, B.W. (Eds.), 1996. Erosion and sediment yield: a global overview, Erosion and sediment yield: global and regional perspectives 236. IAHS (International Association of Hydrological Sciences) Press, Wallingford, UK, pp. 3–19.
Walsh, J.P., Corbett, R., Kiker, J., Orpin, A., Hale, R., Ogston, A., 2014. Spatial and temporal variability in sediment deposition and seabed character on the Waipaoa River margin. Continental Shelf Research, New Zealand.
Warner, J.C., Sherwood, C.R., Signell, R.P., Harris, C.K., Arango, H.G., 2008. Development of a three-dimensional, regional, coupled wave, current, and sediment-transport model. Comput. Geosci. 34 (10), 1284–1306.
Warrick, J.A., Milliman, J.D., 2003. Hyperpycnal sediment discharge from semiarid southern California rivers: implications for coastal sediment budgets. Geology 31 (9), 781–784.
Warrick, J.A., Xu, J., Noble, M.A., Lee, H.J., 2008. Rapid formation of hyperpycnal sediment gravity currents offshore of a semi-arid California river. Cont. Shelf Res. 28 (8), 991–1009.
Wheatcroft, R.A., 1990. Preservation potential of sedimentary event layers. Geology 18 (9) 843–843.
Wheatcroft, R.A., 2000. Oceanic flood sedimentation: a new perspective. Cont. Shelf Res. 20 (16), 2059–2066.
Wheatcroft, R.A., Drake, D.E., 2003. Post-depositional alteration and preservation of sedimentary event layers on continental margins, I. The role of episodic sedimentation. Mar. Geol. 199, 123–137.
Wheatcroft, R.A., Wiberg, P.L., Alexander, C.R., Bentley, S.J., Drake, D.E., Harris, C.K., et al., 2007. Post-depositional alteration and preservation of sedimentary strata. In: Nittrouer, C.A., Austin, J.A., Field, M.E., Kravitz, J.H., Syvitski, J.P.M., Wiberg, P. L. (Eds.), Continental Margin Sedimentation: From Sediment Transport to Sequence Stratigraphy 101–155. International Association of Sedimentologists, Blackwell Publishing Ltd., Oxford, UK.
Wiberg, P.L., 2000. A perfect storm: formation and potential for preservation of storm beds on the continental shelf. Oceanography 13 (3), 93–99.
Wood, M.P., 2006. Sedimentation on a high input continental shelf at the active Hikurangi margin (M.S. thesis). Victoria University of Wellington, Wellington, New Zealand.
Wright, L.D., Friedrichs, C.T., 2006. Gravity-driven sediment transport on continental shelves: a status report. Cont. Shelf Res. 26, 2092–2107.
Wright, L.D., Nittrouer, C.A., 1995. Dispersal of river sediments in coastal seas: six contrasting cases. Estuaries 18 (3), 494–508.